frontiers | Frontiers in Earth Science

TYPE Original Research
PUBLISHED 02 September 2025
DOI 10.3389/feart.2025.1638088

OPEN ACCESS

EDITED BY
Manoj Khandelwal,
Federation University Australia, Australia

REVIEWED BY
Hasan Tosun,
Turkish Society on Dam Safety, Türkiye
Zhenkui Gu,
Chinese Academy of Geological Sciences (CAGS), China
Qing Yang,
University of Wisconsin–Milwaukee, United States
Dinesh Kumar Sahadevan,
National Geophysical Research Institute (CSIR), India

*CORRESPONDENCE
Dinara Talgarbayeva,
turebekova.d.n@gmail.com

RECEIVED 30 May 2025
ACCEPTED 28 July 2025
PUBLISHED 02 September 2025

CITATION
Talgarbayeva D, Vilyaev A, Dedova T, Kuznetsova O and Jangulova G (2025) InSAR monitoring of dam deformations in a seismically active region of Kazakhstan for identifying precursors of failure.
Front. Earth Sci. 13:1638088.
doi: 10.3389/feart.2025.1638088

InSAR monitoring of dam deformations in a seismically active region of Kazakhstan for identifying precursors of failure

Dinara Talgarbayeva*, Andrey Vilyaev, Tatyana Dedova, Oxana Kuznetsova and Gulnar Jangulova

Laboratory of Hydro-Environmental Modeling, Institute of Ionosphere, Almaty, Kazakhstan

Assessing the condition of hydraulic structures (HS) is critical to minimizing the risks to the population and infrastructure in the event of their collapse. HS in seismically active regions are particularly hazardous, as natural and man-made factors can combine to cause catastrophic consequences. This paper analyzes the causes of the Voroshilov Reservoir dam breach (Kazakhstan, a seismically active region, March 2024) using Satellite Radar Interferometry (InSAR) and Ground Penetrating Radar (GPR) profiling. InSAR revealed a persistent upward trend in dam deformations (amplitude over 30 mm since spring 2022), presumably associated with swelling of waterlogged soil. GPR data obtained 2 months after the reservoir was drained confirmed abnormally high moisture content throughout the dam, indicating chronic filtration and the development of internal erosion. A moderate correlation was found between deformations and microseismic activity in the region. It was concluded that the combination of high filtration, soil instability, microseismicity and structure wear led to the accident. Our research shows that a wavy pattern of displacements with a sharp increase in amplitude in earthen dams is a key indicator of critical moisture saturation, forewarning a breach or failure. Furthermore, unstable deformation dynamics during seismic events are also a crucial sign for monitoring dams in earthquake-prone areas.

KEYWORDS

InSAR, monitoring, dam deformation, dam breach, ground penetrating radar (GPR), LIDAR, seismic activity

1 Introduction

Dams play a crucial role in regulating water resources, providing hydroelectric power, irrigation, water supply, and flood protection. However, like any engineering structures, they are subject to wear and tear, natural impacts, and human errors. The breach of a dam can lead to catastrophic consequences, including the flooding of populated areas, loss of life, destruction of infrastructure, and environmental damage.

There are hundreds of thousands of small dams and tens of thousands of large dams and reservoirs in operation worldwide, and their number continues to grow steadily. Despite the obvious socio-economic benefits that such structures provide, including power generation, water supply, flow regulation and flood protection, dam failures still occur. The causes of these incidents are varied: from engineering miscalculations and foundation defects to reservoir overflows, seismic impacts, and failure of spillway systems. Since dam failure

poses a serious threat to the lives of people and infrastructure, issues of prevention and preparedness for such events are of key importance. Although catastrophic failures are relatively rare, their scale of destruction can be colossal. According to the International Commission on Large Dams (ICOLD), by 2025 there will be about 58,700 large dams in operation worldwide (International Commission on Large Dams, 2020). At the same time, about 3,000 accidents of varying severity are recorded annually at hydraulic structures.

The most dangerous of these are accompanied by the destruction of the dam and the sudden release of a significant volume of water, which causes large-scale flooding of adjacent territories. An additional concern is that a significant portion of the operating dams were built decades ago and are already approaching the end of their standard service life. Common causes of dam failure include foundation and structural defects (as in the case of the Malpasset Dam accident in France in 1959), overflow of reservoirs and overflow over the crest, internal filtration and cavitation processes leading to erosion of the dam body (an example is the Teton Dam disaster in the USA in 1976), seismic impacts, design and operational errors, as well as man-made or natural emergencies, including military actions and rock falls in the water area. The history of hydraulic engineering structures operation knows many tragic examples: the destruction of the Gleno Dam in Italy (1923) and the St. Francis Dam in the USA (1928) was caused by a combination of design flaws and overflow. One of the largest man-made disasters of the 20th century was the destruction of the Banqiao-Shimantan dam cascade in China in 1975, which resulted in a gigantic flood and numerous human casualties, estimated at tens of thousands (Aureli et al., 2021). This circumstance increases the requirements for technical monitoring; diagnostics of structures and detection of hidden defects associated with the aging processes of materials.

There are more than 1,502 hydraulic structures (HS) in Kazakhstan, including 247 dams, 461 weirs, 405 reservoirs, 271 ponds and 118 hydraulic complexes of various departmental affiliation and forms of ownership. 24% of large HS are in republican ownership, the rest are on the balance sheet of municipal, industrial and agricultural enterprises. Small HS are a serious problem, some of which are abandoned, have no owners or operating service. Their technical condition is extremely unsatisfactory. The annual damage from the unsatisfactory condition of regulating and protective structures from the harmful effects of water - from floods, floods, flooding - is estimated at tens of millions of US dollars throughout the country. Thus, one of the largest floods in the last 80 years occurred in the spring of 2024 in Kazakhstan, which lasted about 2 months and led to the breakthrough of dams and levees in the western region of the country. Floods affected 10 regions of the country. In total, 224 settlements and 17,603 residential buildings were damaged because of floods.

Today, both ground-based and remote research tools are used to monitor hydraulic structures. Ground-based monitoring includes visual control by specialists, GPR (Huang et al., 2024; Loperte et al., 2011; Tanajewski and Bakuła, 2016; Xue et al., 2023), geodetic (Acosta et al., 2018; Gikas and Sakellariou, 2008; Kalkan, 2014; Nestorović et al., 2024), instrumental (use of sensors and automatic observation systems) (Tang et al., 2019; Wang P. et al., 2020), hydrological (monitoring of water levels, filtration, groundwater) (Allias Omar et al., 2022; Betti et al., 2021) and automated (Leigh et al., 2019; Nasika et al., 2022) research. The advantage of ground-based research is the ability to obtain highly accurate data on deformations directly in the area where the monitoring equipment is located. However, its limitation is the discrete nature of measurements with a low point density, which makes it difficult to obtain a complete picture of the deformation process throughout the entire study area. Therefore, remote sensing demonstrates the successful application of technologies for determining the condition of dams and dikes, allowing for effective monitoring of deformations, subsidence, and other changes in the hydraulic structures (Bayaraa et al., 2022; Jänichen et al., 2025; MacChiarulo et al., 2021; Marchamalo-Sacristán et al., 2023; Pang et al., 2023; Wang et al., 2020b). Despite the effectiveness of each approach, the combination of ground and remote sensing allows for comprehensive monitoring of the technical condition of structures, timely detection of potentially dangerous deformations and minimization of accident risks through operational data analysis.

This study is aimed at identifying spatio-temporal patterns of deformations of the Voroshilov Reservoir dam, located in a seismically active region, using the InSAR method to detect signs preceding failure. To validate the results obtained and demonstrate the effectiveness of the method, as well as a control object, the paper also presents the results of a similar analysis of the Priyut Reservoir dam, located in the same region, but not subject to failure and having no signs of an accident preceding it.

The main research method in our work is Interferometric Synthetic Aperture Radar (InSAR), which over the past decades has been gaining popularity and application in various areas of monitoring of hydraulic structures [dams and levees, hydroelectric power plants (Dwitya et al., 2024)], urban development objects (high-rise buildings and residential complexes (Liu et al., 2023; Ma et al., 2022; Yang et al., 2016), bridges (Guzman-Acevedo et al., 2024), subways (Li et al., 2025)), transport infrastructure [railways (Koohmishi et al., 2024), highways (Fan et al., 2024), airports (Xiong et al., 2024)], industrial facilities [mines and quarries (Abdikan et al., 2014; Ng et al., 2024; Zheng et al., 2024), oil and gas infrastructure (Pengchao, 2025)] and geologically active and hazardous zones [landslide areas (Tian et al., 2025), seismic (Bayramov et al., 2024) and volcanic areas (L. Wang et al., 2024)].

In turn, InSAR offers 2 methods for monitoring displacements: Differential Interferometric Synthetic Aperture Radar (DInSAR) and Multi-Temporal Interferometric Synthetic Aperture Radar (MT-InSAR). We use the MT-InSAR method, which allows analyzing a large number of time series of radar images while tracking slow and long-term deformations of the earth's surface with high accuracy (up to millimeters per year). In turn, MT-InSAR has two modifications: permanent scattering interferometry (PSI) (Crosetto et al., 2016) and the small baseline subset (SBAS) (Aditiya and Ito, 2023). Both modifications use stacks of numerous SAR images, while highlighting points with high coherence and stability of reflection in time series, defining them as reference points. Phase changes in reference points are analyzed based on the corresponding phase models, which allows effectively compensating for the influence of atmospheric delay and obtaining more accurate information on deformations of the earth's surface. The growing recognition of MT-InSAR in monitoring hydraulic structures is supported by the results of studies conducted by

the world scientific community. For example, the authors Zhiguo Pang et al. (Nasika et al., 2022) used the SBAS method to assess the current stability of a dam and identify potentially dangerous areas that require additional attention and possible strengthening. The paper (Ruiz-Armenteros et al., 2021) proposes a model based on machine learning algorithms that can predict potential dam deformations based on historical radar data using the PSI processing method. Miguel Marchamalo-Sacristán et al. (MacChiarulo et al., 2021) presented an integrated approach to monitoring the Beninar earth dam in Spain using two MT-InSAR methods and numerical modeling. The integrated approach provided a more complete and accurate understanding of the deformation processes occurring in the dam. All the authors of the studies suggest using InSAR as an effective tool for regular monitoring of hydraulic structures, which helps to improve their safety and durability.

2 Materials and methods

2.1 Study area

The Voroshilov Reservoir is located on the Zharmukhamet and Boraldai Rivers in the village of Baikent, Almaty Region, Kazakhstan. It was first commissioned in 1910 for the irrigation of 580 ha. In 1970, the dam body was reconstructed with concrete lining of the upper and lower pools. The reservoir dam is an earth dam 180 m long and 8.5 m high with reinforced concrete reinforcement. The volume of the reservoir at the normal headwater level (NBL) is 1.36 million m^3 at an elevation of 610 m. To regulate the flow of water into the reservoir, there are 4 spillways with a capacity of 2.6 m^3/s. The actual volume of the reservoir immediately before the breakthrough, according to the Water Resources and Irrigation Department of the Almaty Region, was about 700,000 m^3, i.e. 50% of the total volume. On 30 March 2024, at 15:50 Astana time, the dam collapsed. Water suddenly gushed along the main channel of the Zharmukhamet River, freely flowing into a cascade of ponds with open sluices. The instantaneous filling of the underlying reservoirs, including two lakes of the Zharmukhanbet River, created a flood threat for more than 12 thousand residents of two settlements, requiring the emergency evacuation of part of the population. To comparative analysis, the Priyut Reservoir, which has similar basic parameters, was studied. Located 10 km southeast of the Voroshilov Reservoir above the village of Tyumebayeva on the Terenkara River (Almaty Region), it was commissioned in 1910 at the same time as the Voroshilov Reservoir and was also reconstructed and strengthened in 1970. It is intended for irrigation of 289 ha and functions in a cascade with other reservoirs. The reservoir capacity at the normal water level is 2.94 million m^3 at a mark of 663 m. The earth dam is 364 m long, 13 m high and 6 m wide along the crest. The upper pool is reinforced with reinforced concrete slabs. The crest of the dam is used as a section of the Almaty-Mezhdurechensk operational highway, which creates a high vibration load on its body.

An overview map of the location of the reservoirs and their technical characteristics are presented in Figure 1 and Table 1, respectively.

The physical and mechanical properties of the soils of the dam body and its foundation were studied using monoliths (soil samples of undisturbed structure) collected at intervals from boreholes driven along the crest and in the lower pool of the dam. According to engineering and geological surveys in 2020, it was established that the dam body is composed of loams from solid to fluid plastic consistency, which are underlain by coarse sands with gravel and pebbles (Figure 2).

Analysis of the seismic regime in the dam area. According to modern data (Silacheva et al., 2018), the probability of exceeding the peak ground acceleration (PGA) of 0.28 g in this area is 10% over 50 years (return period of 475 years). However, when designing the dam, a horizontal acceleration coefficient corresponding to 0.22 g was included, taking into account the soil conditions. In this case, the stability factor was determined as 1.056. We assume that the structural properties of the dam do not meet modern safety standards for seismic loads.

As part of this study, a detailed analysis of the seismic regime of the area adjacent to the dam was carried out, covering the period from 2017 to 2024. Monitoring showed that 50 weak earthquakes with a maximum magnitude not exceeding M = 2.0 were registered within a radius of 30 km from the structure. It is noteworthy that most of these events (77%) had hypocenters at depths of 5–10 km, which is typical for crustal earthquakes. In addition to local microseismicity, more significant events were noted. During the analyzed period, two noticeable earthquakes with magnitudes of M = 4.4 and M = 5.5 occurred within 70 km from the dam. Particular attention is paid to the Akkol earthquake with a magnitude of M = 7.0, which occurred on 22 January 2024 in China. Although the distance to it was about 320 km from Almaty, its impact was felt in the city with an intensity of up to 5 points on the Mercalli macroseismic scale. Given the linear dimensions of the dam, the seismic impact from all recorded earthquakes (both local and distant) can be approximated as uniformly distributed across its individual sections. This assumption allows for an analysis of the response of the entire structure to seismic loads without focusing on a point impact.

2.2 Methods

2.2.1 GPR

To study dam deformations and detect failure precursors, the ground penetrating radar (GPR) method was used. It can detect hidden defects, water-saturated zones and heterogeneities in embankment dams and dikes. The method is based on the analysis of changes in the electrical conductivity and permittivity of the soil, which affect the stability of hydraulic structures (Davis and Annan, 1986).

Ground profiling along the dam crest was carried out using the OKO-2 ground penetrating radar with an AB-400 shielded antenna (central frequency 400 MHz, maximum probing depth 6 m, depth resolution 0.25 m). The surveys were carried out in clear sunny weather to minimize radargram distortions caused by an increase in permittivity by wet soil (up to 10–20 times).

The obtained data were processed and interpreted using the GeoScan32 software. Primary processing of radargrams included the application of second-level mathematical procedures aimed at optimizing the signal-to-noise ratio: inverse filtering, bandpass filtering, horizontal filtering, aperture synthesis, envelope extraction, spectral field, signal smoothing, and

10.3389/feart.2025.1638088

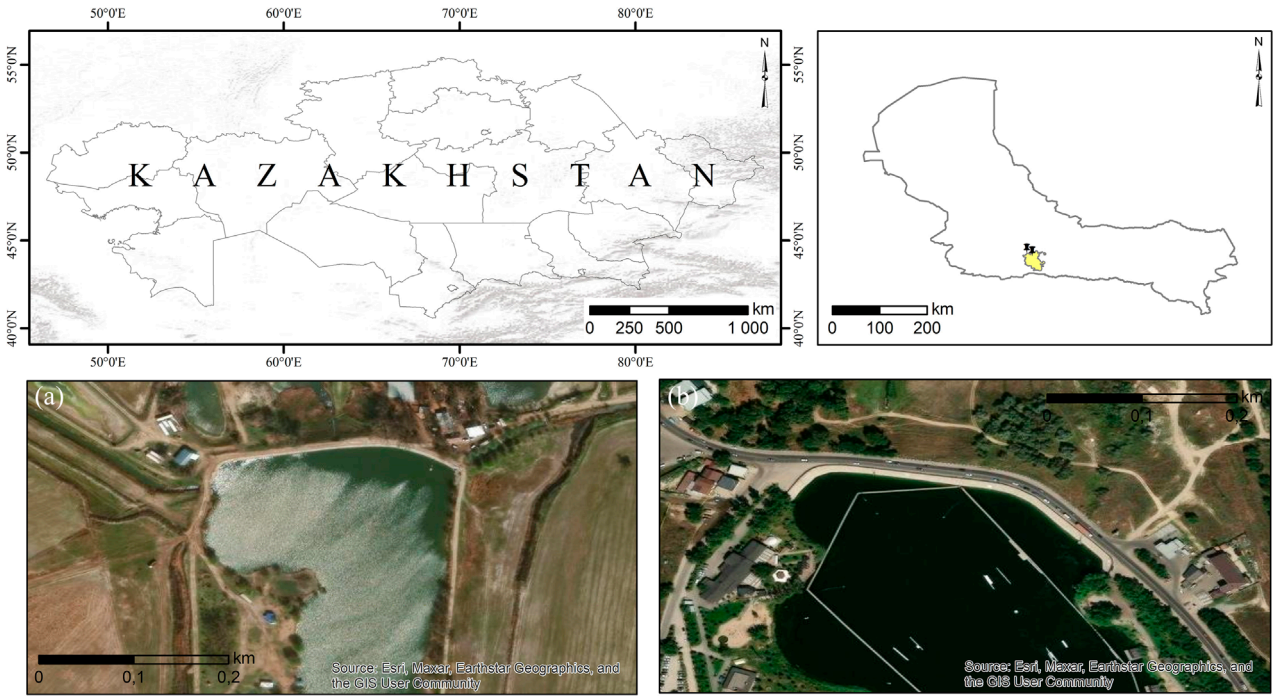

FIGURE 1
Overview map: **(a)** Voroshilov Reservoir and **(b)** Priyut Reservoir.

TABLE 1 Technical characteristics of dams.

Name	Voroshilov	Priyut
Year of Establishment	1910	1910
Type of Reservoir	Cascade	Cascade
Dam Type	Earthen	Earthen
Volume, million m3	1,36	2,94
NPL Elevation, m	610	663
Length, m	180	364
Height, m	8,5	13
Crest Width, m	6	6
Upstream Slope Facing	Reinforced concrete slabs, 0.5 thousand m2	Reinforced concrete slabs, 0.5 thousand m2
Upstream/Downstream Slope Ratio	2:1/2:1	2.5:1/2:1
Height Above Sea Level	645 m	666 m

contour extraction. The result of these operations was a "clean" radargram with clearly expressed inhomogeneities of the dam soil foundation.

The conversion of radargram time scales to depth was performed using average dielectric permittivity values typical for slightly saturated light loams ($\varepsilon \approx 9$) and coarse-grained sands with gravel ($\varepsilon \approx 5$), based on standard calibration tables and soil composition data for the study area.

It should be noted that the interpretation of zones with increased moisture content in this study is qualitative (relative) in nature and is primarily based on variations in signal amplitude and the continuity of reflective horizons.

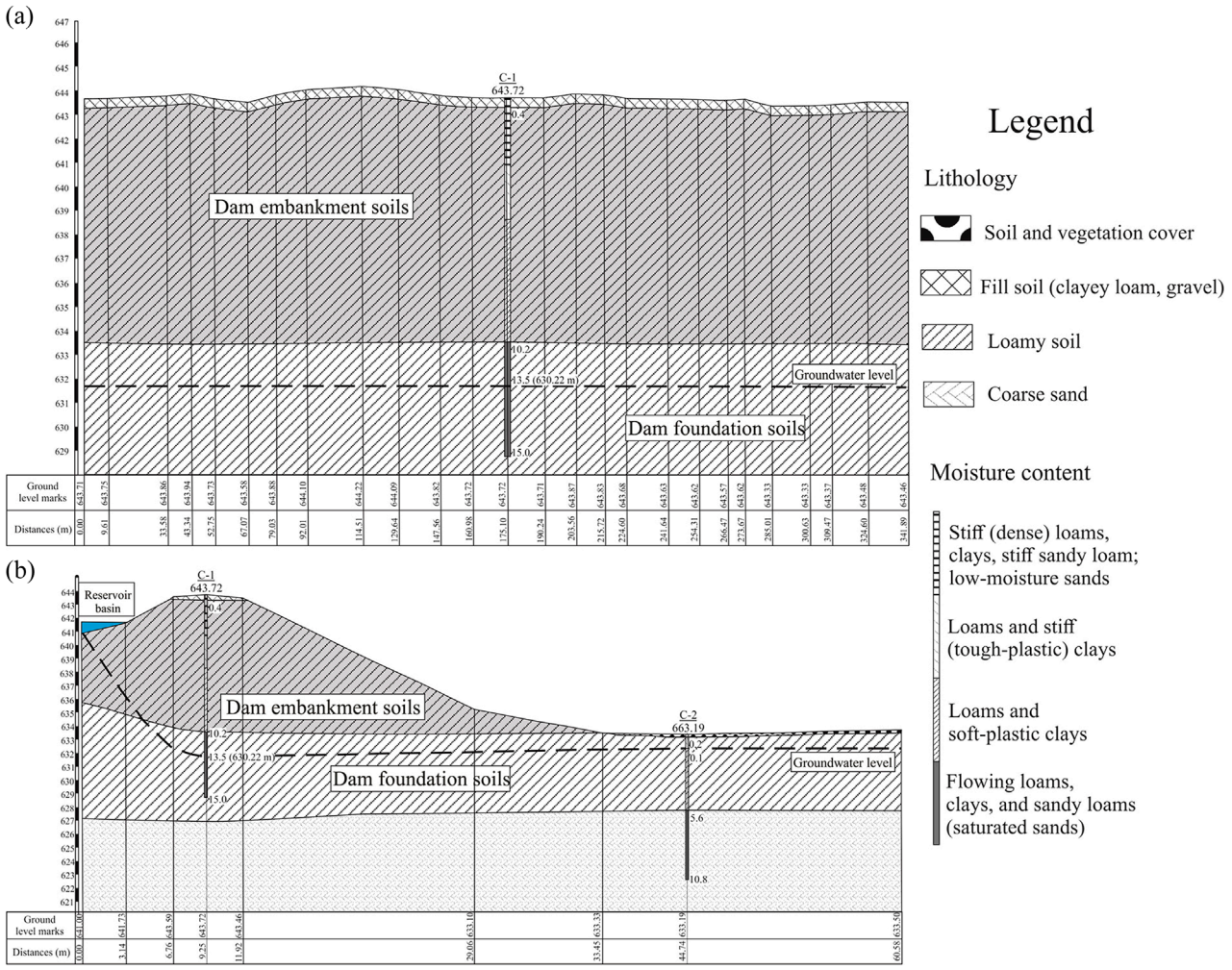

FIGURE 2
Geological and lithological section of the Voroshilov reservoir dam: **(a)** along the dam axis, **(b)** along the dam cross-section axis of the Voroshilov reservoir.

We acknowledge that soil dielectric permittivity is directly dependent on moisture content, and that quantitative assessment of its spatial distribution requires the use of specialized inversion methods, which are beyond the scope of the current study.

2.2.2 InSAR

In this study, Sentinel-1A satellite data covering the period from 15 March 2017 to 10 June 2024 were used. A total of 155 ascending and 151 descending orbit images collected during the snow-free period (mid-March to late November) were analyzed. These radar images in the SLC IW C-band format (5.6 cm wavelength, 20 m azimuth and 5 m radius spatial resolution) are freely available for download after registration from the Alaska Satellite Facility (ASF) website (https://asf.alaska.edu/).

For high-precision monitoring of dam deformations, the SBAS-InSAR method implemented in the Sarscape (ENVI) software package (https://www.nv5geospatialsoftware.com) was used. SAR provides all-weather, 24-h vertical and horizontal displacement data collection, while InSAR processing captures vertical and horizontal motion, providing millimeter-level surface motion quantification (Hanssen, 2001), minimizing the subjectivity of visual analysis. The SBAS-InSAR method used in this work includes automatic coregistration, interferogram calculation and filtering, orbital parameter correction (GCP), phase inversion to reconstruct displacement history and geocoding of results (Figure 3).

The analysis was performed using VV vertical polarization and two independent sets of Sentinel-1A images in ascending and descending orbits. Temporal and spatial baseline thresholds were set to optimize the number of interferometric pairs generated. Given the characteristics of the studied area, in particular dense vegetation, building density and seismic instability, a 48-day baseline was chosen as a temporal threshold. The spatial baseline was limited to 48% of its maximum possible value, which allowed the formation of 511 and 496 interferometric pairs for ascending and descending orbits, respectively. Previous research has demonstrated that snow cover, especially during melting or drifting phases, can substantially degrade temporal coherence in InSAR data (Ruiz et al., 2022; Zakharov and Zakharova, 2023). Seasonal snowpack changes–due to wind or melting–alter the

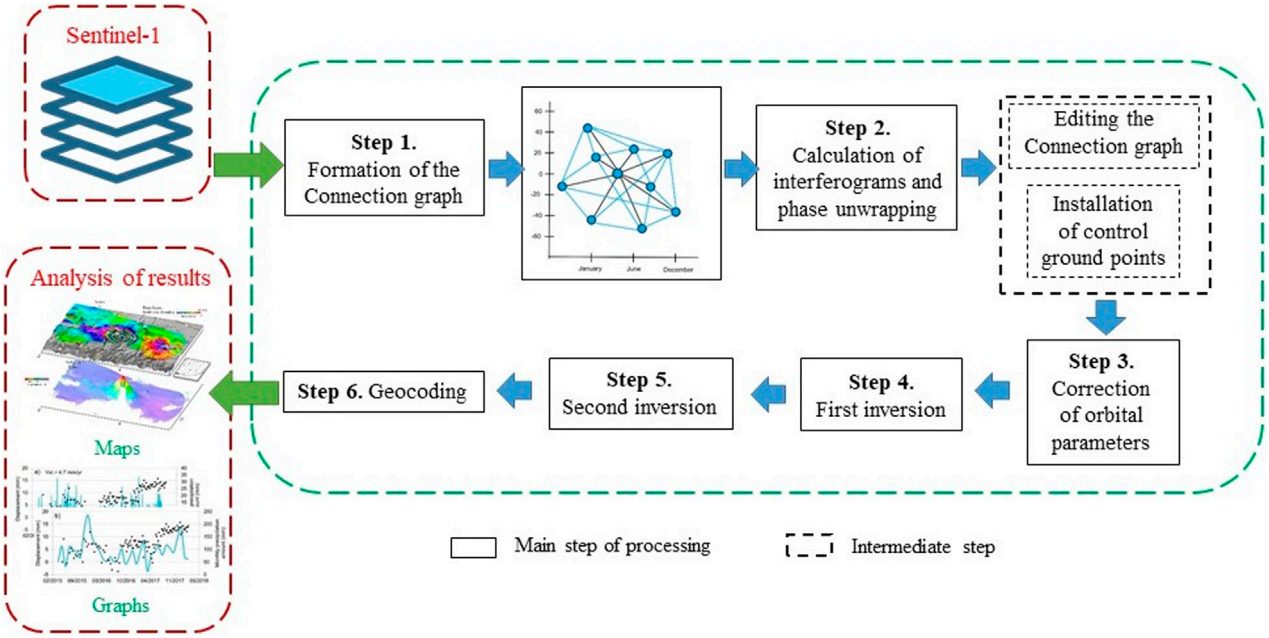

FIGURE 3
Technological chain of processing multipass radar data using SBAS methods of SARscape.

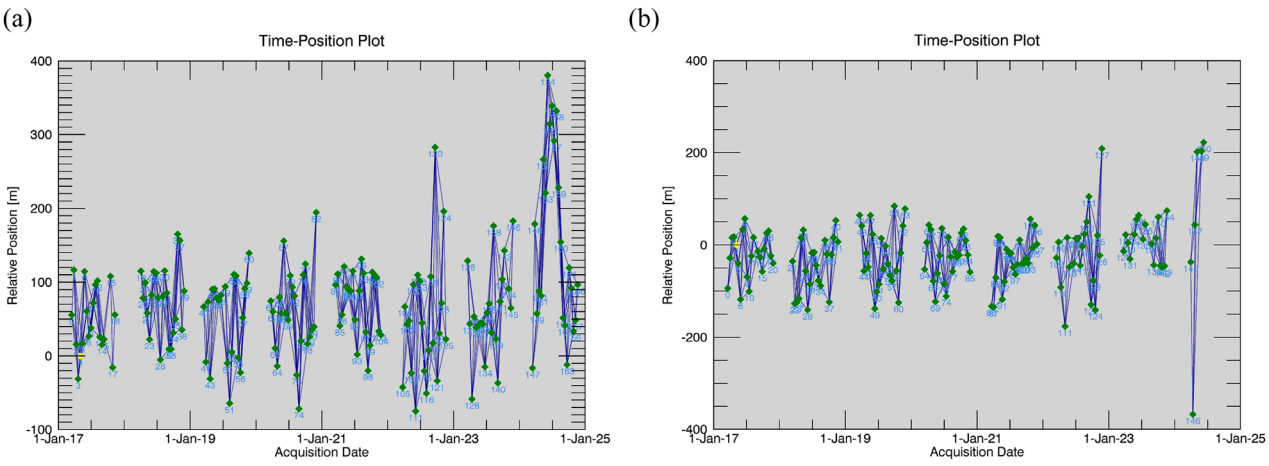

FIGURE 4
Spatiotemporal baseline SBAS-InSAR: **(a)** – ascending and **(b)** – descending.

phase delay and scattering properties of the surface, leading to decorrelation, especially in C and X-band sensors. In our study, winter acquisitions were excluded to avoid such decorrelation effects, ensuring high coherence during snow-free periods and improving the robustness of deformation analysis. Although the concept of a fully connected temporal baseline network is generally recommended for SBAS processing, seasonal data gaps due to snow cover made this impractical in our case. To address this, we enabled the "Allow Disconnected Blocks" option in SARscape (Figure 4).

The output file of the processing results is a georeferenced raster file of the velocity of displacement (LOS).

3 Results

3.1 Reconstruction of the geometric parameters of the dam breach using an unmanned aerial vehicle and LIDAR technology

As part of the integrated monitoring program of the Voroshilov Reservoir, preceding the GPR, a detailed aerial survey was conducted using a DJI Matrice 350 unmanned aerial vehicle equipped with a Zenmuse L1 lidar scanner. The purpose of this survey was to create a high-precision 3D model of the terrain around

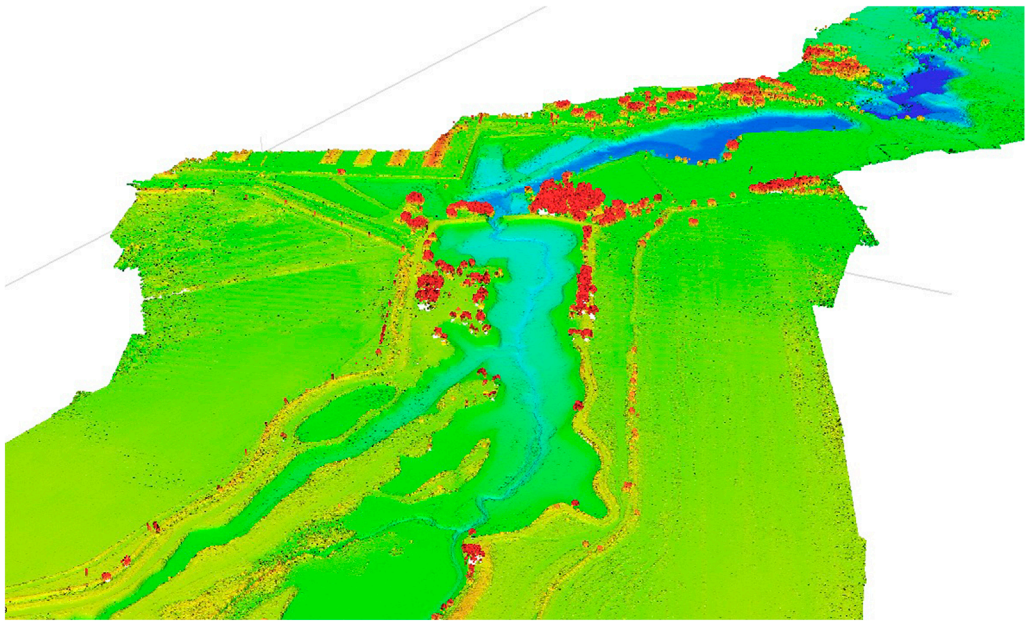

FIGURE 5
Digital terrain model (DTM) of the Voroshilov reservoir.

the dam breach and subsequent analysis of the geometric parameters of the resulting breach.

The Zenmuse L1 lidar is a multifunctional surveying instrument that combines a LiVOX lidar module, an inertial measurement system (IMU) with high accuracy of position and orientation determination, and a camera with a 1-inch CMOS sensor mounted on a 3-axis stabilized suspension. This integration ensures efficient acquisition of spatial 3D data with high detail and accuracy.

The aerial lidar survey was conducted on 6 June 2024, from a variable drone flight altitude in the range from 30 to 150 m above the surface. Analysis of the obtained DTM showed that the actual volume of water outflow was 472,000 m^3 (67% of the original volume), which is due to the retention of part of the water by the natural rise of the bottom in the southern part of the reservoir. (Figure 5). In addition, the DTM analysis made it possible to determine the geometric characteristics of the gap with high accuracy: the width of the upper part is 25 m, the lower part is 3 m, the vertical height is 10 m (Figure 6). The obtained quantitative parameters are key for further analysis of the causes of destruction and assessment of potential risks.

3.2 Analysis of dam water saturation based on GPR

To determine the state of the dam body of the Voroshilov and Priyut hydraulic structures (HS), an analysis of their water saturation was carried out using the ground penetrating radar (GPR) method. Based on the survey results, 25 profiles were obtained for the Voroshilov Reservoir (Figure 7a) and 39 profiles for the Priyut Reservoir (Figure 7b).

GPR of the Voroshilov and Priyut reservoirs, conducted on 7 June 2024, in order to obtain data on the subsurface structure, revealed anomalous zones of increased moisture saturation in the dam body.

In the presented radargrams, the zones of increased moisture saturation are marked with black ovals (see Figures 8–10). In the radargrams, the horizontal scale reflects the profile length (in meters), the left vertical scale - the propagation time of the radio signal in nanoseconds (ns), the right scale - the recalculated depth in meters (m). On the right is a color scale of signal intensity, calibrated by the degree of water saturation of the medium.

During the survey of the Priyut reservoir, no significant or critical zones of decompression in the dam body were found. The intensity of moisture saturation in the decompression zones is shown on the GPR profiles by a color scale from minimum (red) to maximum (blue) (Figure 8). Localized areas with increased moisture saturation are recorded, which may be due to lithological features of the soil or local variations in moisture. Analysis of longitudinal profiles No. 003 with a length of 73.8 m (Figure 8a) and No. 009 with a length of 64.2 m (Figure 8b) demonstrates that the penetration depth of moisture saturation zones in some areas reaches 2 m.

The destroyed dam of the Voroshilov Reservoir is a special object for detailed GPR analysis. Profiles obtained in the immediate vicinity of the breakthrough zone (No. 056 on the left, 30.3 m long, and No. 042, 34.9 m long, on the right, Figures 9a,b respectively) demonstrate extensive areas of moisture saturation, traced almost along the entire length of the profiles and reaching a depth of up to 2 m in some areas.

FIGURE 6
3D model of the Voroshilov reservoir dam breach, obtained by lidar surveying.

Ground penetrating radar profiles taken along the lower edge of the dam to the left (profile No. 063, 44.5 m, Figure 10a) and to the right (profile No. 43, 30.6 m, Figure 10b) of the breach site demonstrate almost continuous zones of moisture saturation along their entire length.

According to engineering and geological surveys, the dam foundation consists of light loams (from semi-solid to flow-plastic), under which coarse sands with an admixture of gravel and pebbles lie. Zones of increased moisture saturation, identified by GPR at a depth of up to 2 m, correspond to fill soils (loam, gravel). Deeper, the dam body is represented by loams. Noteworthy is the moderate moisture saturation at a depth of 4–5 m in certain areas to the west of the ravine, which differs from the surrounding areas (Figures 9a, 10a).

3.3 Analysis of dam deformation processes

The analysis of deformation processes of the dam was carried out. The results of InSAR monitoring of deformations of the Voroshilov Reservoir (Figures 11, 12), visualized on a high-resolution orthophoto map, revealed spatially heterogeneous deformation behavior. On a small-sized dam (~180 m × 6 m in size), 10 coherent points were identified on the ascending orbit and 8 on the descending orbit using the SBAS method for displacement analysis; a coherence threshold of 0.7 was applied during data processing, which ensured the reliability of the estimates by excluding all points with lower values from the analysis.

The analysis of the displacement rate over 8 years (ascending orbit, Figure 11b) showed active upward displacement in the western part, moderate positive displacement in the breakthrough zone and stability in the eastern part. The time schedule of displacements (Figure 11c) demonstrates a complex deformation pattern with interannual and seasonal variations.

The analysis of displacement velocities obtained from the descending orbit (Figure 12b) revealed more stable values recorded in the western part of the dam, moderate positive displacement in the breach zone, and subsidence across the entire eastern section of the dam.

The opposite signs of the line of sight (LOS) offsets obtained from the ascending and descending orbits indicate the presence of a pronounced horizontal offset component oriented predominantly in the east-west direction. Combining the two-orbit observations allowed us to quantitatively decompose the offsets into vertical and horizontal components, which provided a more detailed understanding of the nature of the earth's surface deformations (Figure 13).

To provide an in-depth interpretation of the revealed deformation anomalies of the Voroshilov dam and to determine the precursors of its failure, a comparative analysis of the behavior of similar hydraulic structures was performed (Figure 14). The Priyut reservoir was chosen as a relevant analog due to the similarity of its technical, design, geological and operational parameters with the Voroshilov reservoir. This allows it to be used to model deformation processes and assess the risks of hydraulic structure failure in similar conditions.

InSAR monitoring of the Priyut dam in the ascending orbit clearly shows the presence of subsidence deformations, concentrated mainly in its eastern part. Over 8 years, cumulative displacements along the line of sight (LOS) reach −35 mm (Figure 15a). The subsidence rate is up to −5 mm/year (Figure 15b).

The graph of time displacements shows a stable linear trend with a tendency towards negative values, which indicates a stable downward displacement of the surface over time (Figure 15c).

In contrast to the results obtained for the ascending orbit, interferometric processing of Sentinel-1A satellite images for the descending orbit shows the opposite picture. Positive displacement velocities are recorded along the entire length of the dam, with maximum values concentrated in its eastern part. LOS

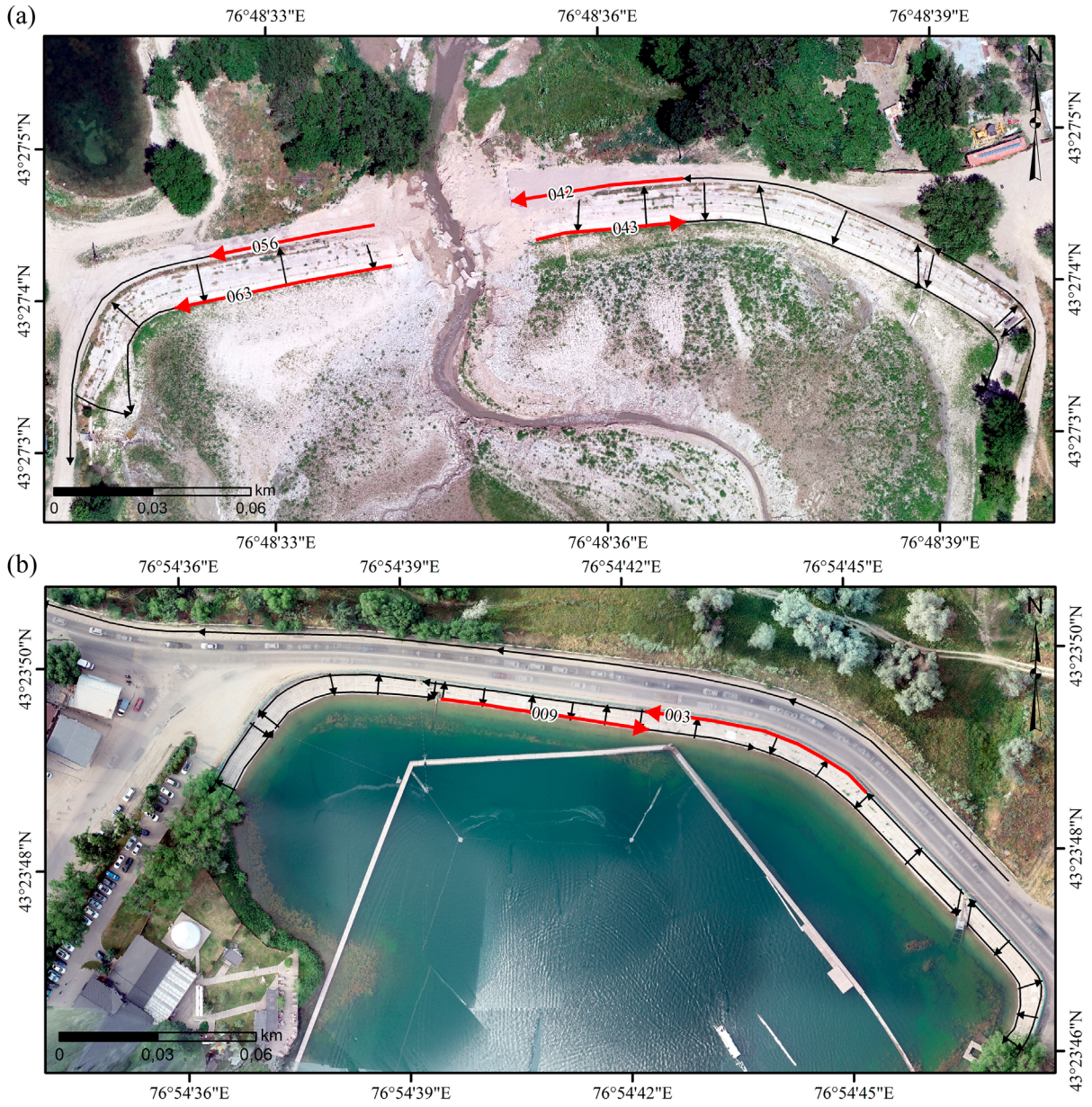

FIGURE 7
Map of the location of ground penetrating radar profiles at the Voroshilov **(a)** and Priyut reservoirs **(b)**.

displacements reach +35 mm in 8 years (Figure 16a), and the subsidence rate is more than 6 mm/year (Figure 16b).

For the Priyut Reservoir, the displacements were also decomposed into vertical and horizontal components based on a combined analysis of ascending and descending orbit data, which made it possible to quantitatively assess the direction and magnitude of deformations (Figure 17).

The results of SBAS-InSAR monitoring in ascending and descending orbits for other similar dams in this region are shown in Figures 18, 19, respectively.

A similar nature of subsidence deformations is demonstrated by the graphs of displacements of the Priyut Reservoir and dams No. 1 and 4 (Figures 18, 19). It is noteworthy that until the spring of 2020, the displacement values remained relatively stable, after which a sharp increase in negative values is observed for the ascending orbit.

Analysis of the time series of deformations of dams No. 2, 3, and 5 (Figures 18, 19) showed insignificant linear displacements within ±20 mm over an 8-year observation period, which indicates a stable behavior of these GTS without pronounced deformation changes.

4 Discussion

The obtained results made it possible to identify a few key processes and potentially dangerous factors.

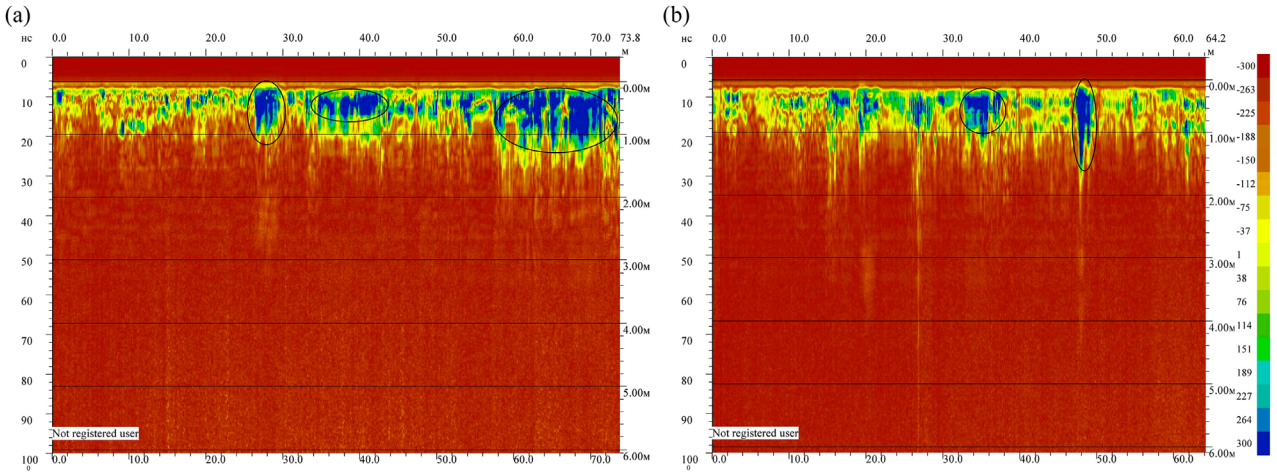

FIGURE 8
Ground penetrating radar profiles along the upper edge of the Priyut reservoir dam: **(a)** №003, **(b)** №009.

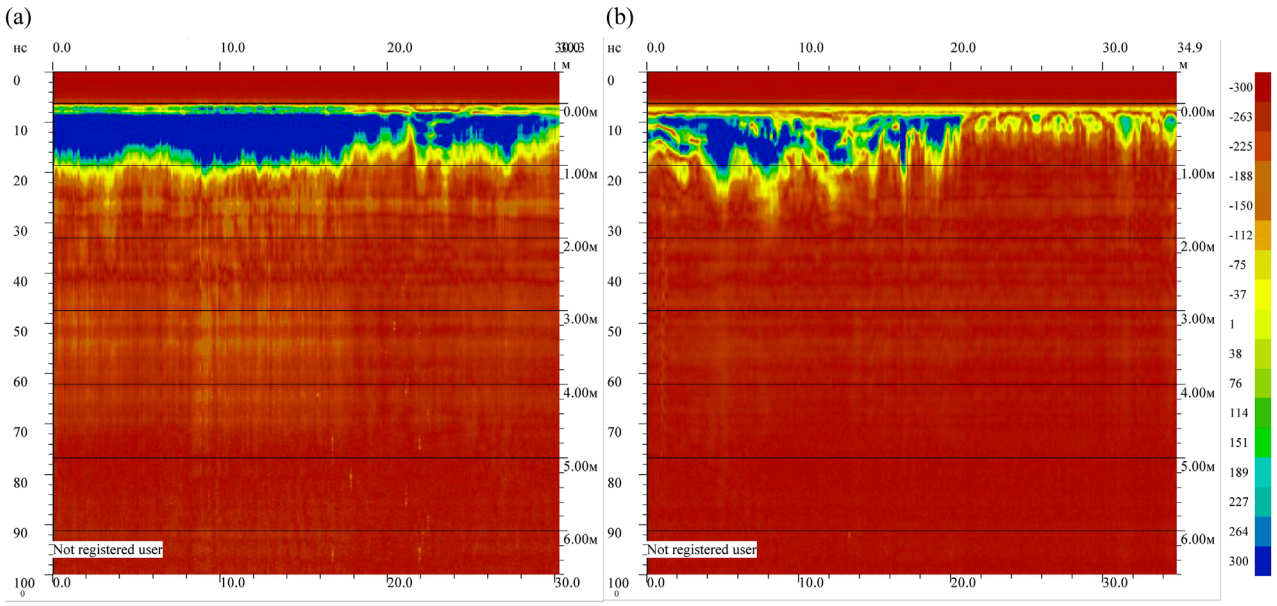

FIGURE 9
Ground penetrating radar profiles along the upper edge of the Voroshilov reservoir dam: **(a)** №056 (left of the breach), **(b)** №042 (right of the breach).

GPR. Anomalies of increased water saturation of the Voroshilov and Priyut reservoirs, recorded by GPR, may indicate the development of internal erosion processes or hidden filtration channels, which critically weakens the dam structure.

Quantitative assessment of radargrams made it possible to determine the depth and extent of these local anomalies, interpreted as signs of soil loosening. At the same time, the analysis of meteorological data (https://rp5.kz) showed that moderate precipitation in Almaty, recorded on 26 May 2024, preceded the survey by 12 days earlier and could not be the main cause of the observed soil moisture.

For the Priyut reservoir (see Figure 8), signs of active filtration through the dam body were not detected at the time of the survey, which indicates the preservation of satisfactory waterproofing properties of the material. At the same time, the presence of these anomalous zones indicates the need for a comprehensive engineering-geological assessment of the dam since they may be indicators of hidden defects or processes that pose a significant potential threat to the structural stability of the structure.

For the Voroshilov Reservoir (see Figure 9) The local decrease in humidity recorded on profile #042 along the upper edge near the steep part of the dam is probably due to the slope exposure, which contributes to the intensification of evaporation processes.

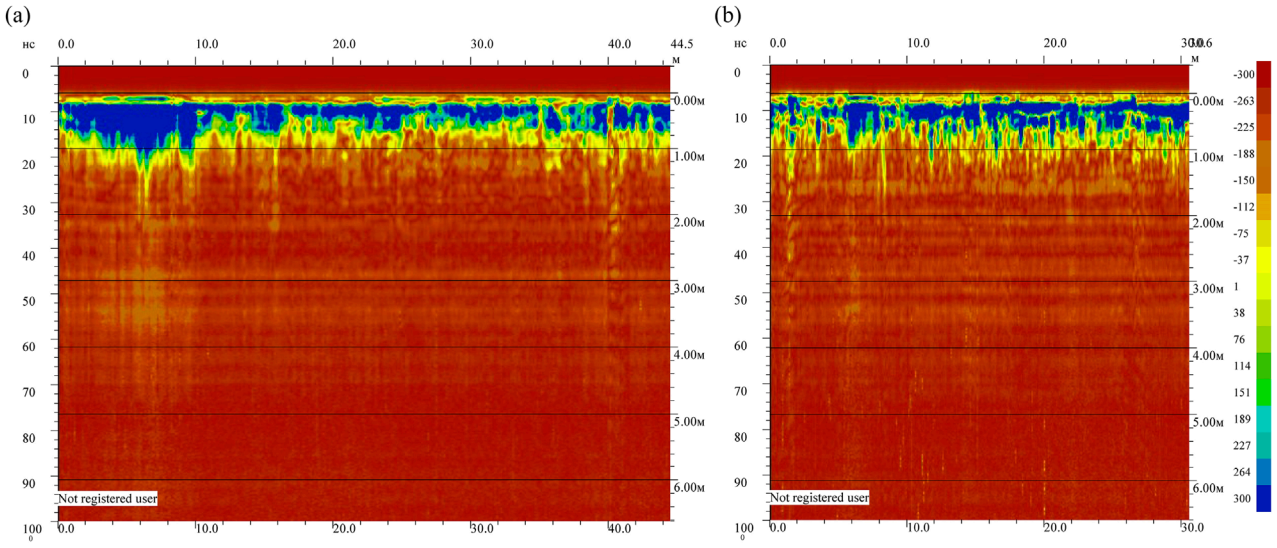

FIGURE 10
Ground penetrating radar profiles along the upper edge of the Voroshilov reservoir dam: **(a)** №063 (left of the breach), **(b)** №043 (right of the breach).

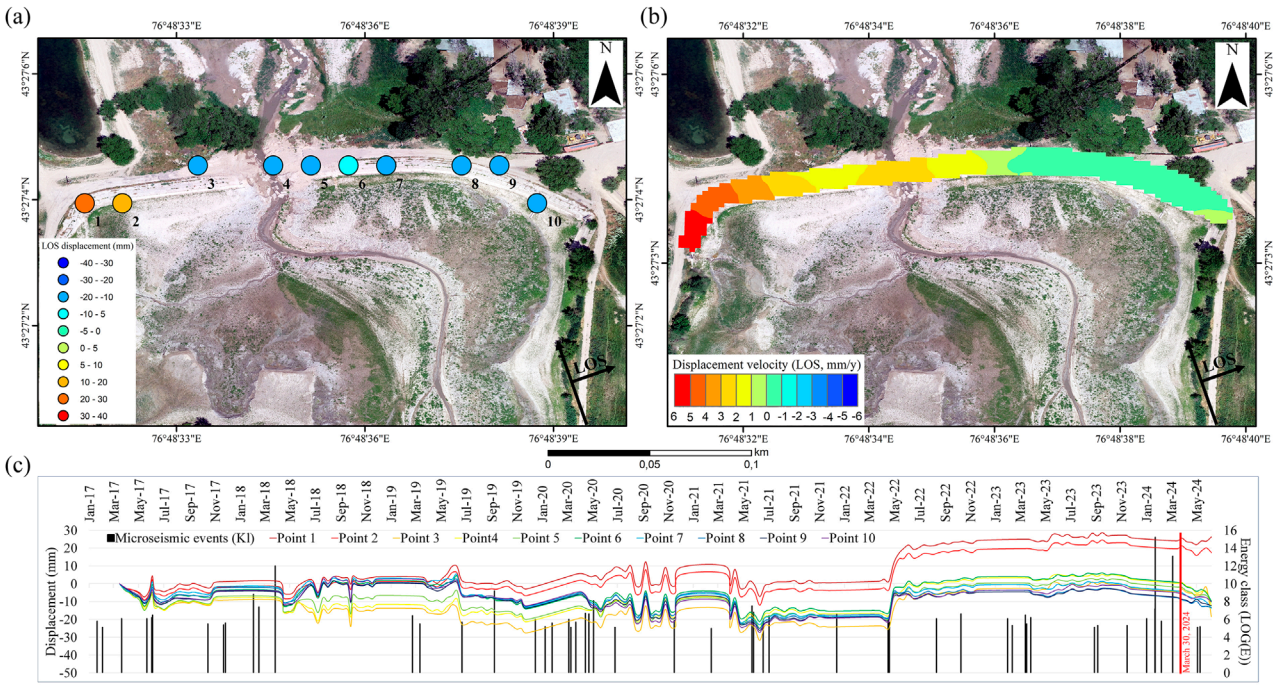

FIGURE 11
Results of SBAS-InSAR monitoring (ascending orbit) of the Voroshilov reservoir: **(a)** LOS displacement points (mm) on 06.06.2024, **(b)** LOS displacement velocities (mm/year), **(c)** LOS displacement time series (mm) for points on the dam and microseismicity.

Considering that the survey was conducted 2 months after the accident in hot season conditions, the observed decrease in humidity most likely reflects the process of surface drying.

For ground penetrating radar profiles along the lower edge of the Voroshilov e Dam (see Figure 10) Considering that these profiles were initially located below the water level, the detected moisture saturation anomalies, which persist more than 2 months after the breakthrough and drying of the dam body, may indicate an initially high level of humidity. This, in turn, suggests the presence of intense filtration processes in the lower part of the dam body, caused by the movement of pore water from the upper pool to the lower pool under the influence of hydrostatic pressure. The GPR results demonstrate high efficiency in assessing moisture saturation and identifying potentially hazardous areas in dams

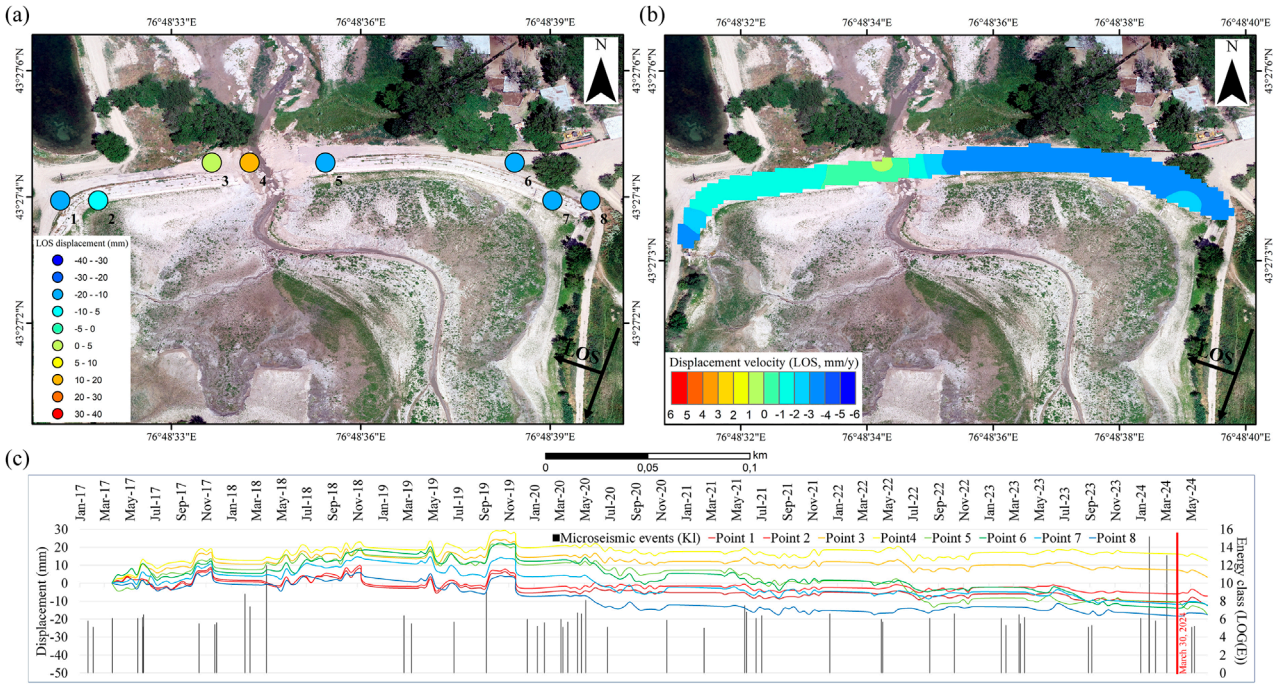

FIGURE 12
Results of SBAS-InSAR monitoring (descending orbit) of the Voroshilov reservoir: **(a)** LOS displacement points (mm) on 10.06.2024, **(b)** LOS displacement velocities (mm/year), **(c)** LOS displacement time series (mm) for points on the dam and microseismicity.

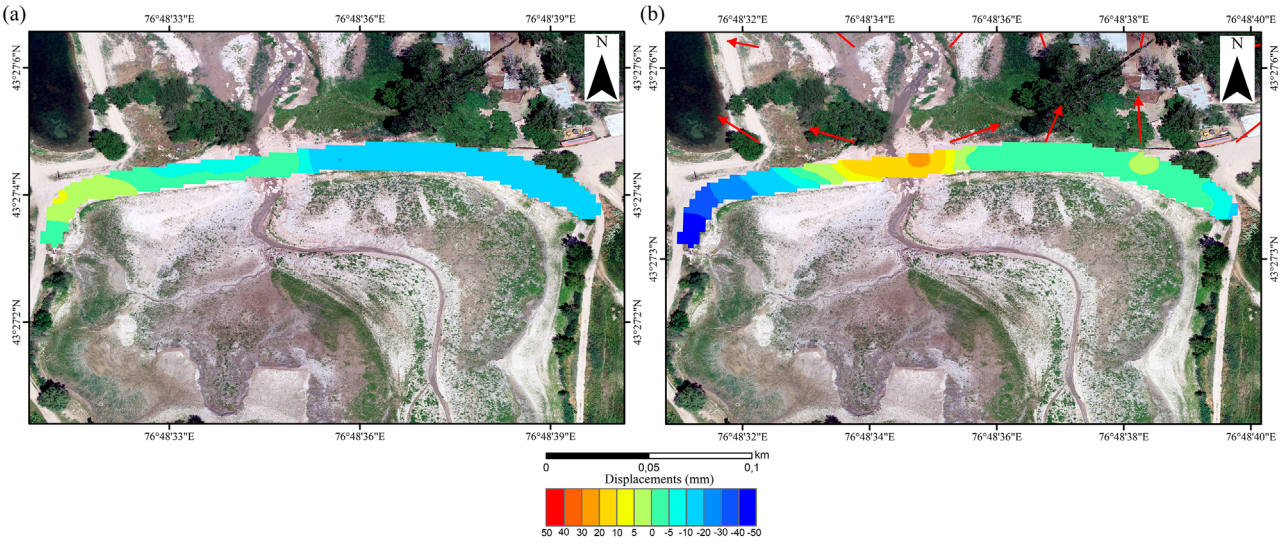

FIGURE 13
Maps of quantitative decomposition of LOS displacements into vertical **(a)** and horizontal **(b)** components and projected horizontal displacement vectors in plan for the Voroshilov Reservoir (red arrows).

subject to filtration processes, which is consistent with the data of previous studies. In particular, the study by Dyakov (2022) revealed anomalies in the electromagnetic signature that correlate with filtration flows in the enclosing dam of the tailing's storage facility. Similarly, Zhantayev et al. (2013) identified areas of low density and high humidity indicating potential zones of internal erosion during a ground penetrating radar survey of dams in Kazakhstan. In addition, a study from the International Journal of Geophysics (Antoine et al., 2015) demonstrated high accuracy of GPR in localizing water leaks in embankment dams when combined with permeability measurements. Thus, both our results and the generalization of literature data confirm the reliability of GPR as a tool for early diagnostics of hazardous hydrogeological processes capable of triggering emergency destruction of the GTS.

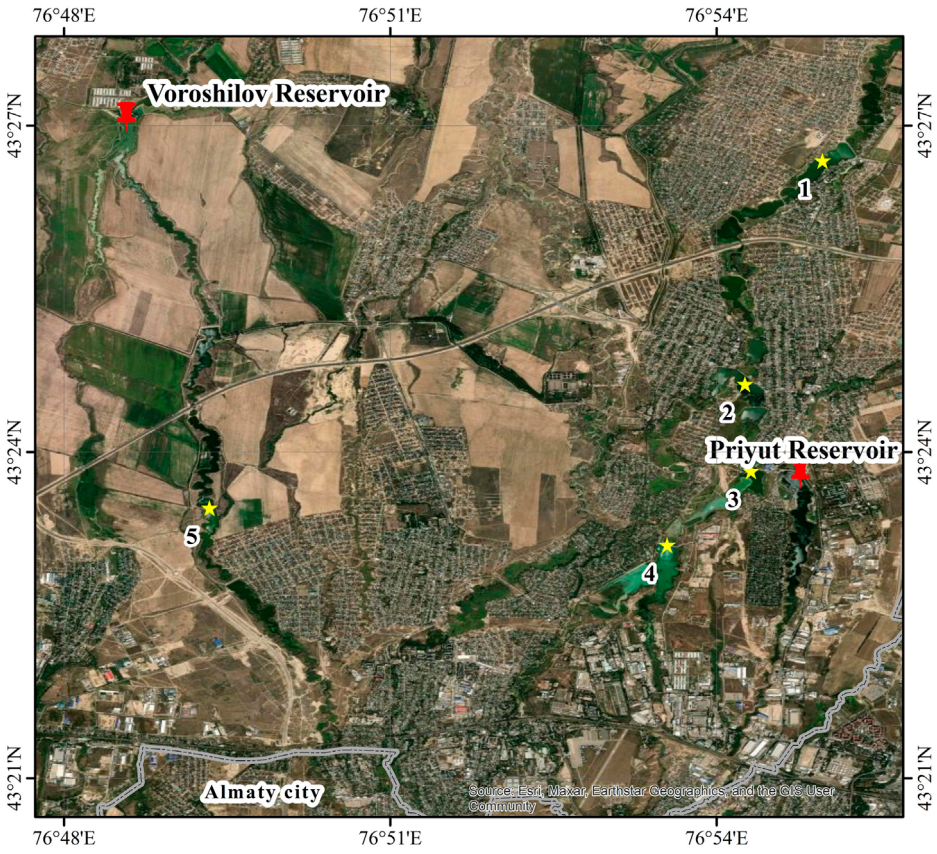

FIGURE 14
Overview map of dams in the Almaty region.

The GPR results for line 003 (Figure 7a) in this zone clearly record abnormally high moisture saturation, which is convincing evidence of active filtration processes and water accumulation inside the dam body. Such anomaly may be an indicator of developing internal erosion or the formation of hidden filtration channels, which in the long term can critically reduce the structural integrity of the structure and lead to its local or complete destruction. The linear nature of the change indicates a constant rate of deformation process, without sharp fluctuations or phase transitions. Such behavior requires additional assessment of the engineering and geological conditions of this zone and may pose a potential threat to the structural stability of the structure.

InSAR monitoring. Analysis of the InSAR monitoring results for the Voroshilov reservoir in the ascending orbit (Figure 11c) showed that Since spring 2022, there has been a stable upward trend in displacements, indicating the activation of deformations, probably due to soil swelling or changes in its water saturation, which is confirmed by GPR data.

At the same time, for the descending orbit Since spring 2022, there has been a stable downward trend in displacements. At the same time, the Time graph of displacements, like the graph for the ascending orbit, reflects the relationship between microseismicity and wave-like deformations.

In the work of Xiao et al. (2022), it is indicated that one of the most common causes of dam failure is water spilling over the crest of the hydraulic structure. However, in the case of the Voroshilov Dam, the breakthrough occurred at a reservoir level of only about 50% of the design capacity, and began in the lower part of the structure, closer to its base. This fact indicates a high vulnerability of the structure even under partial operational load and indicates the presence of hidden structural or geotechnical defects, such as insufficient filtration resistance or weak cohesion of the dam body materials, not detected during the design or operation.

The absence of recorded displacements corresponding to the 26-m breakthrough of the Voroshilov Dam in the Sentinel-1 interferometric data is due to a significant limitation in the spatial resolution of satellite images. The IW mode resolution (20 × 5 m) is insufficient for detailed monitoring of small-scale local deformations, especially if they occur in the intervals between raster grid elements or in areas of sparse reflector coverage. This limitation of Sentinel-1 spatial resolution in monitoring local deformations is confirmed by a number of studies, including those on transport infrastructure (Piter et al., 2024), fast landslides (Tzouvaras et al., 2020) and small-scale deformations revealed by Quasi-PS InSAR (Wang et al., 2020c).

The observed discrepancy between the location of maximum InSAR-detected deformation and the actual breach point is primarily attributed to the spatial distribution of coherent scatterers on the dam surface. Due to the dam's relatively small dimensions, heterogeneous surface materials, and complex geometry, coherent

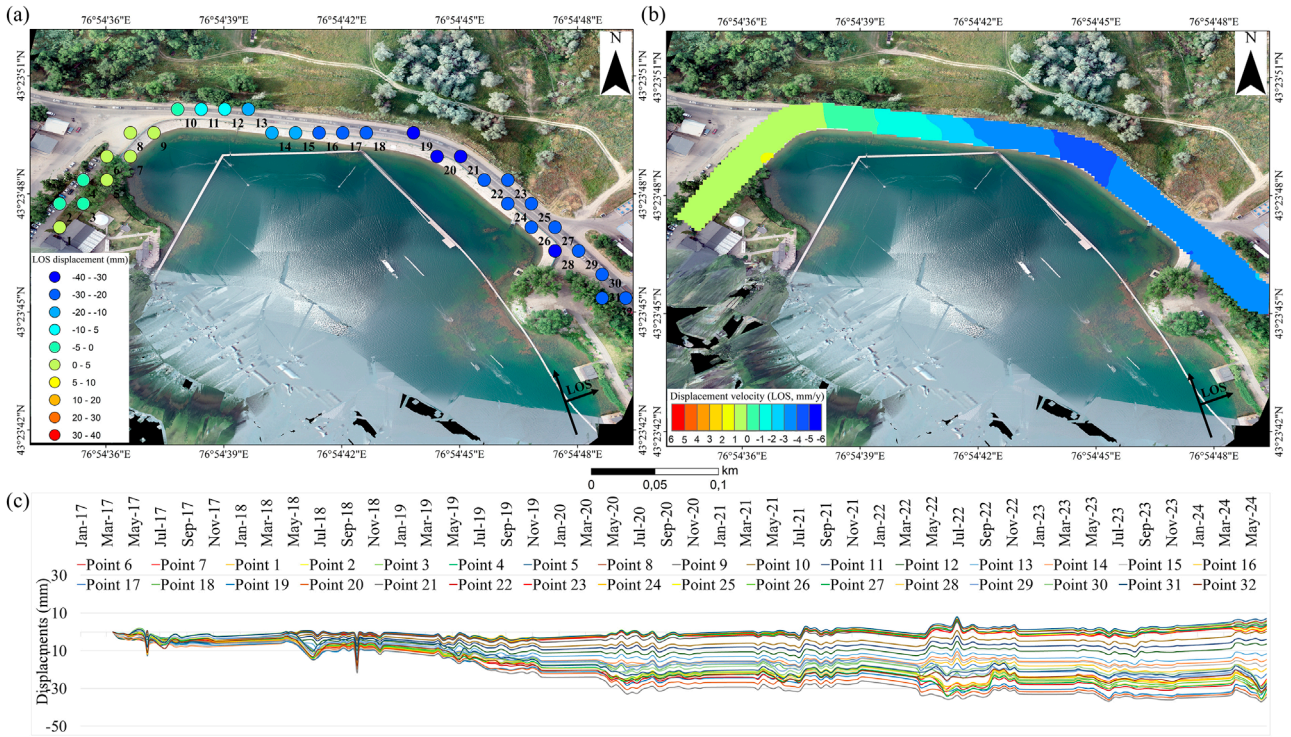

FIGURE 15
Results of SBAS-InSAR monitoring (descending orbit) of the Priyut reservoir. **(a)** LOS displacement points (mm) on 10.06.2024, **(b)** LOS displacement velocities (mm/year), (c) LOS displacement time series (mm) for points on the dam.

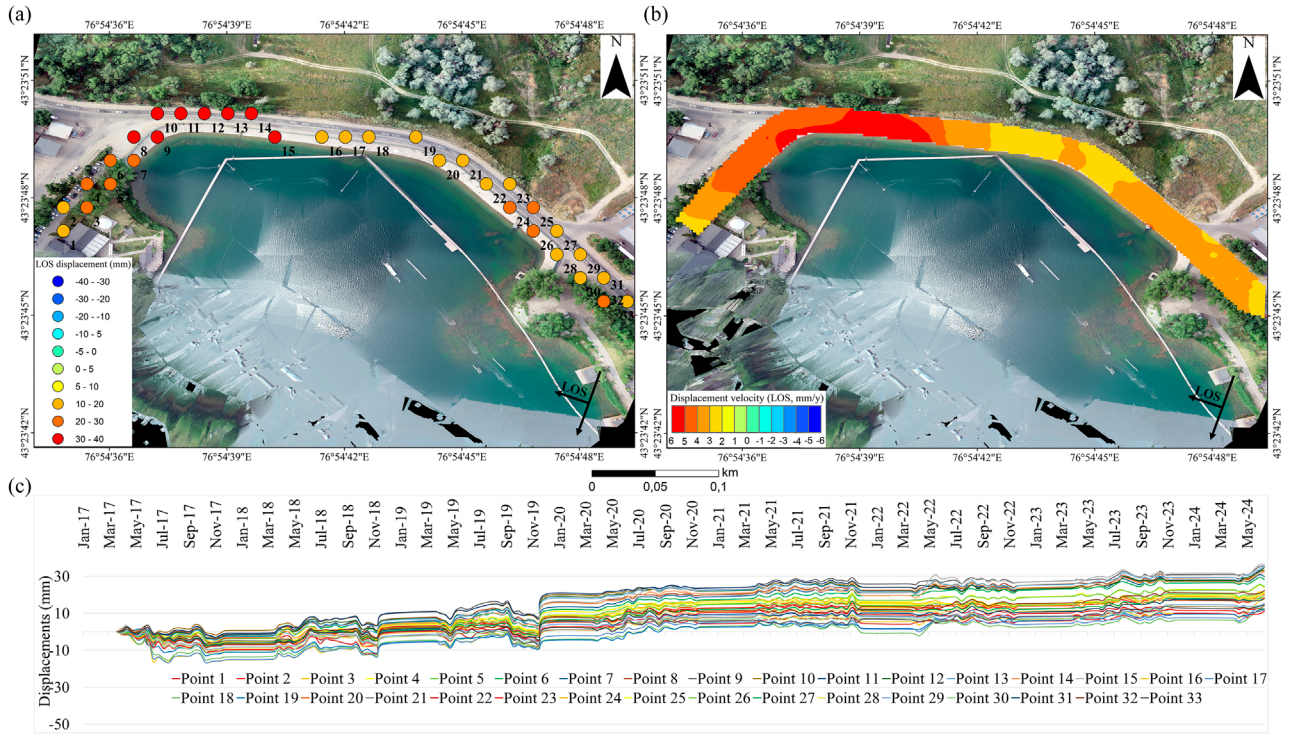

FIGURE 16
Results of SBAS-InSAR monitoring (ascending orbit) of the Priyut reservoir. **(a)** LOS displacement points (mm) on 06.06.2024, **(b)** LOS displacement velocities (mm/year), (c) LOS displacement time series (mm) for points on the dam.

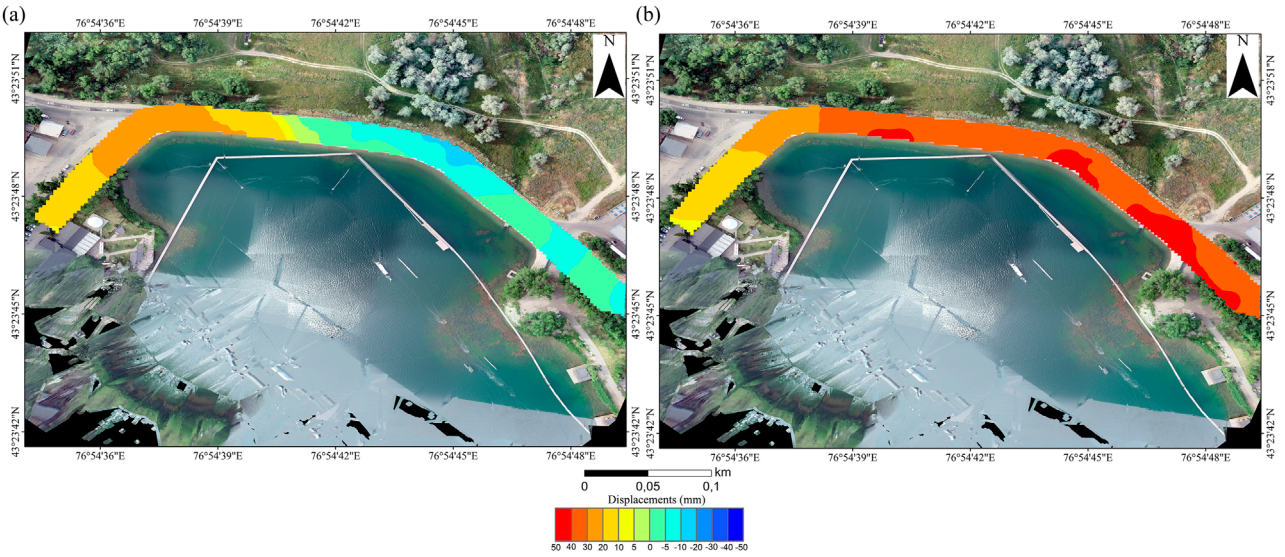

FIGURE 17
Maps of quantitative decomposition of LOS displacements into vertical **(a)** and horizontal **(b)** components of the Priyut Reservoir.

InSAR points are unevenly distributed. Moreover, it is well established that abrupt structural failures often cause a sudden loss of coherence in SAR data, making reliable deformation measurements unavailable at the precise location of collapse. For example, the observations made by the authors during the collapse in the mine (Teixeira et al., 2024), along with studies by researchers who examined the effects of abrupt changes on consistency (Hrysiewicz et al., 2023). Impact of abrupt changes on coherence. In our case, no coherent points were detected exactly at the breach location. However, as shown in Figures 11, 12, several coherent points are located in close proximity to the breach, slightly downstream, and still capture the broader deformation pattern associated with the failure.

In addition, our analysis indicates that the deformation was predominantly horizontal, with opposite displacement vectors observed on either side of the dam crest (Figure 13). This suggests complex internal deformation processes that may have contributed to the structural instability. Therefore, although larger deformation magnitudes were detected on the western section, we conclude that the failure initiated in the central part due to the combination of mechanical weakening, hydraulic loading, and structural asymmetry.

The results of InSAR monitoring for the Priyut Reservoir in the ascending orbit (see Figure 15) with negative offsets indicate ongoing compaction of the soil massif, which may be associated with local filtration or consolidation. A probable factor intensifying these processes is the dynamic impact of heavy traffic on the road located directly on the crest of the dam. Repeated cyclic loads can provoke additional compaction, increase in the filtration coefficient and accumulation of residual deformations, especially in areas with reduced bearing capacity of the soil. The stability of deformations in the western part of the dam, remote from the transport load, convincingly confirms the significant influence of the latter on the deformation state of the Priyut dam. The formation of a pronounced local minimum of displacements in the dam bending zone can be due to the concentration of increased hydrostatic pressure in this area. The geometric configuration of the structure's bend causes an uneven distribution of stresses, which leads to local overloads of individual sections. In combination with the constant pressure effect of water, this can provoke the development of subsidence deformations, which represent a potential threat. Particularly vulnerable are zones with weakened soil strength characteristics and a high degree of water saturation, which intensifies filtration flows and contributes to progressive decompaction of the dam body materials.

Analysis of the InSAR monitoring results for the Priyut Reservoir in the descending orbit (see Figure 16) showed the opposite picture. Calculations of the shifts along the line of sight (LOS) show negative values for the ascending orbit and positive values for the descending orbit. This configuration requires a separate analysis considering the differences in the radar viewing geometry.

The ascending orbit of the Sentinel-1 satellite is oriented from the southwest to the northeast, and the radar scans the territory to the east of the trajectory. In this case, negative LOS shifts indicate the movement of the object towards the radar, i.e., in the easterly direction.

Similarly, in the descending orbit (northwest - southeast), when the radar "looks" to the west, positive LOS shifts reflect movement away from the radar, which also corresponds to the easterly direction of movement. Thus, the simultaneous presence of negative displacements along the ascending and positive ones along the descending orbit can be interpreted as a predominantly horizontal displacement of the studied surface in the easterly direction.

This is confirmed by the quantitative decomposition of LOS displacements into vertical and horizontal components (Figure 16), where a significant predominance of horizontal displacement is clearly visible. Positive values of horizontal displacements indicate a predominantly easterly direction of movement. Over the entire observation period, the dam surface has shifted eastward

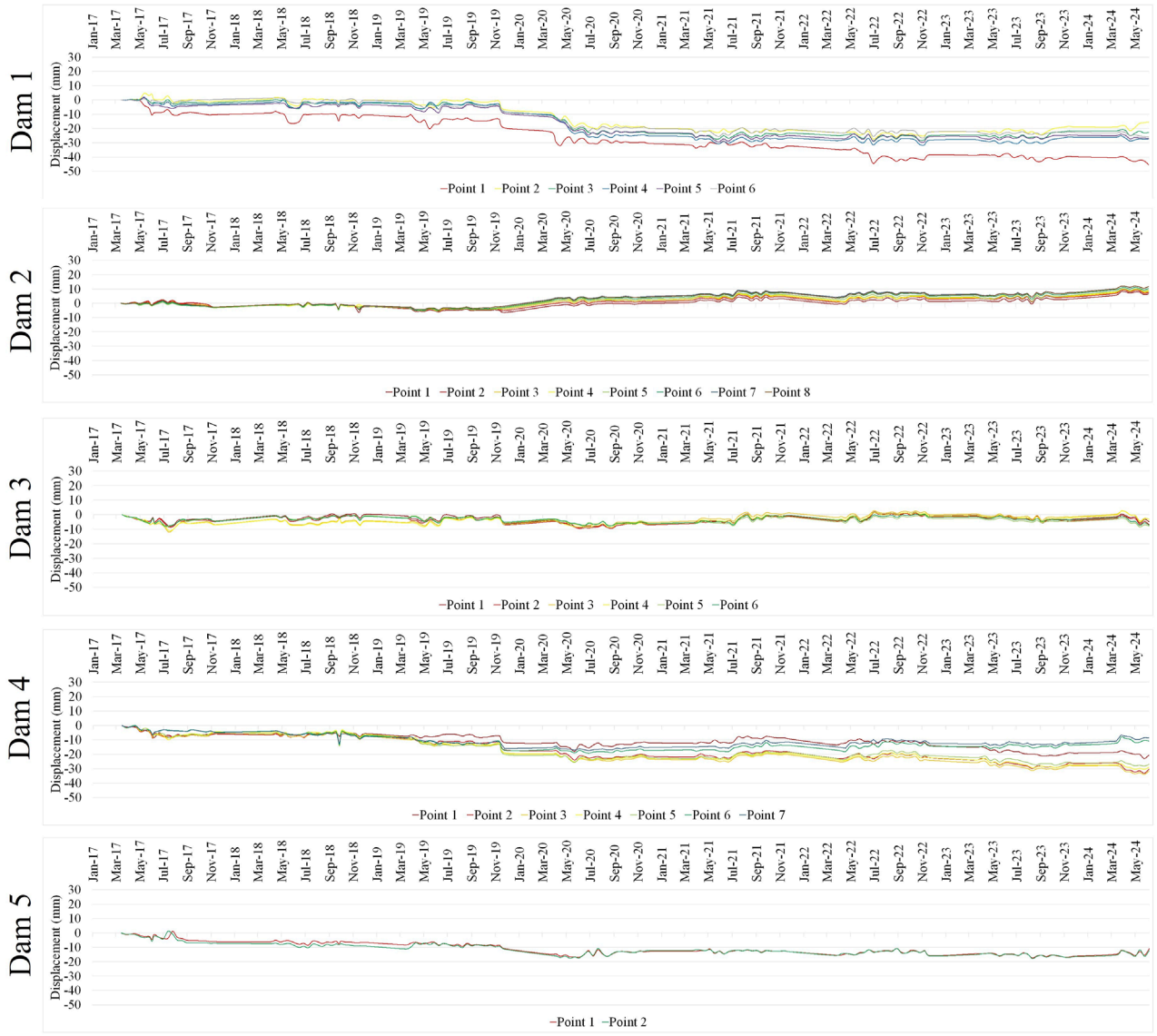

FIGURE 18
Time series plots of dam displacements for the ascending orbit in the Almaty region.

by ~50 mm. In turn, vertical displacements do not exceed ±20 mm, which indicates their secondary role in the overall deformation pattern.

Such differences in LOS displacements observed from the Sentinel-1 ascending and descending orbits are not a contradiction, but, on the contrary, reflect different sensitivity of orbital trajectories to horizontal components of motion. As shown in the work of Hu et al. (2014), InSAR phase information obtained from different viewing directions records projections of the common displacement vector onto the line of sight direction of each satellite. This allows, when combining data from ascending and descending orbits, to reconstruct a three-dimensional displacement field, including horizontal components that cannot be reliably extracted when analyzing a single orbit.

The authors emphasize that the difference in LOS displacements in ascending and descending orbits carries information about the direction and magnitude of horizontal displacements, especially in the east–west plane, and is necessary for the correct interpretation of deformation processes on the surface. Opposite-sign displacements observed in ascending and descending orbit data may be due to the predominance of the horizontal component of motion, which is projected onto the satellite's line of sight differently depending on the orbit direction. A similar effect was demonstrated by Jo et al. (2015), where differences between ascending and descending InSAR results allowed the determination of a three-dimensional deformation field of the Kilauea caldera. Combining these data allowed the authors not only to quantify the vertical and horizontal components of inflation, but also to localize the source of subsurface pressure that was inaccessible to single-sided observation.

Seismicity. The results of InSAR monitoring of 5 additional dams in this region (Figures 18, 19) show a relatively stable deformation pattern, but since 2020, an increase in subsidence has been noted at

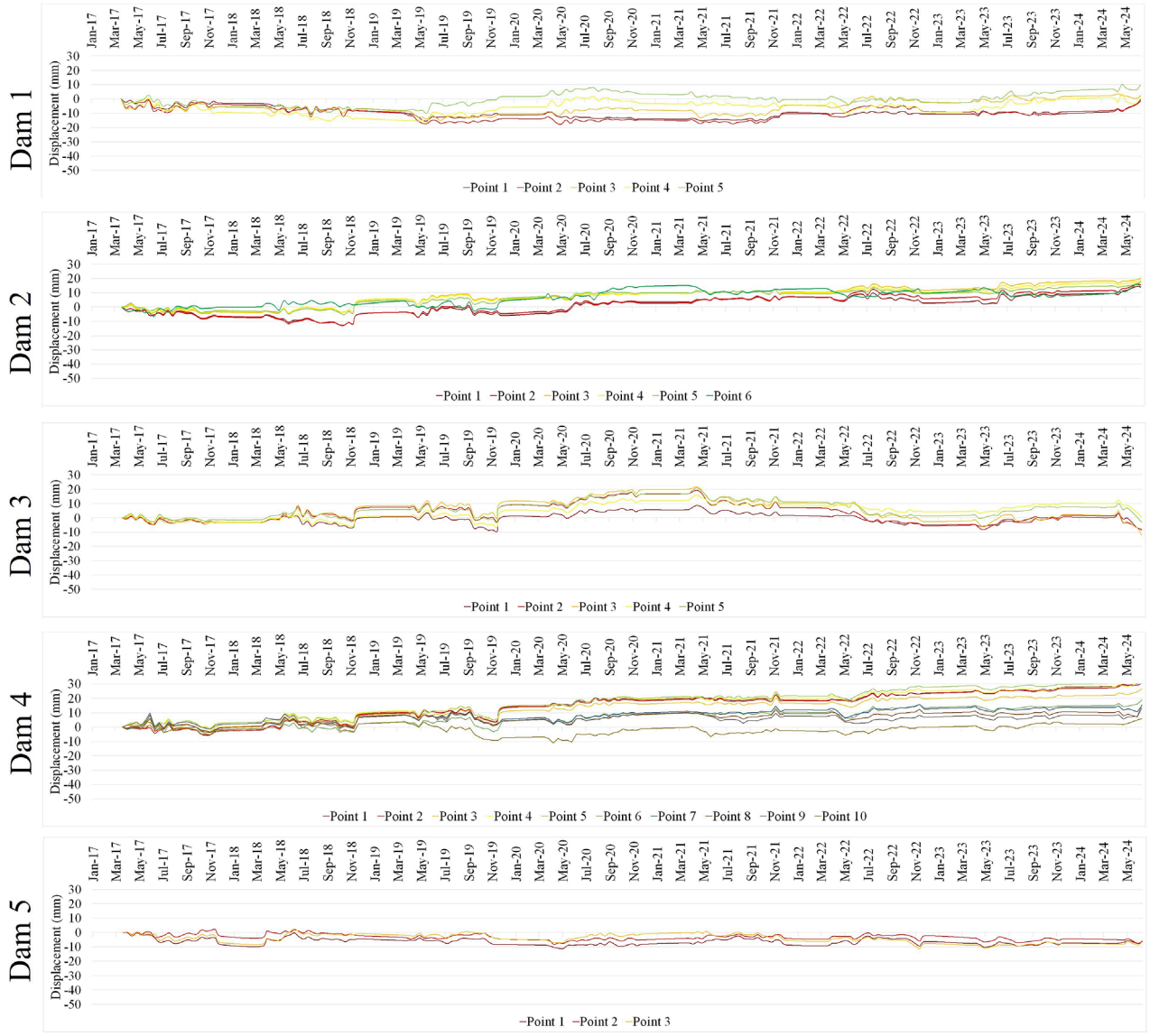

FIGURE 19
Time series plots of dam displacements for the descending orbit in the Almaty region.

a few dams. This activation of deformation processes may be due to a series of successive seismic events, which probably initiated additional stresses in the dam structure, leading to a violation of their previous stability.

A comparative analysis of the relationship between seismic events and dam deformations, performed at a qualitative level, is presented in Figure 20. After the earthquakes that occurred, intense wave deformations of the Voroshilov Reservoir dam were observed with a delay of up to 1 month, lasting from five to 6 months. The observed wave-like nature of the deformations is probably a consequence of the complex interaction of seismic impacts and hydrogeological processes, such as changes in the pore pressure of water, soil consolidation and liquefaction, which have delayed effects. The key mechanism is the development of excess pore pressure in the dam body during an earthquake, as well as its subsequent delayed dissipation.

The increase in pore pressure is due to pore compression under the influence of microseismicity. The dissipation rate of this pressure is inversely proportional to the permeability of the soil, which causes the delayed nature of the deformations. A decrease in the effective normal stress due to pore pressure, with an unchanged shear stress, contributes to the development of deformations. An additional factor is the creep of the dam material, which is a slow, long-term deformation under a constant load, which can manifest itself over months or years. It should be noted that similar wave-like deformations were not observed for the Priyut dam during the same time period. We believe that the wave-like deformations of the dam are the result of a complex interaction of seismic dynamics, poroelasticity and rheological properties of the soil massif.

To assess the statistical significance of the relationship between the time of seismic events and deformation changes in the dam, considering the discrete and abnormal nature of the temporal

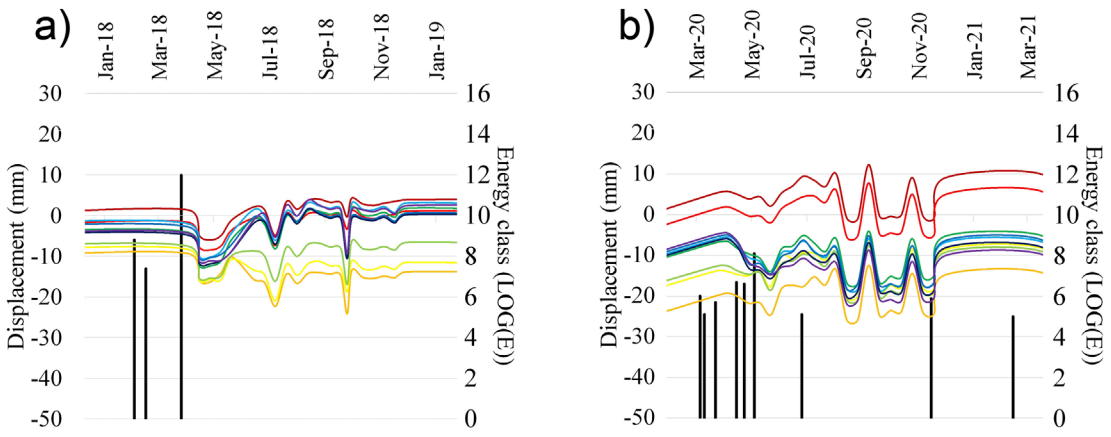

FIGURE 20
Analysis of the relationship between seismic events and deformations of the Voroshilov Reservoir dam: **(a)** 2018 and **(b)** 2020.

distribution of earthquakes, a nonparametric correlation analysis based on the Spearman Rank Order Correlation coefficient was used. The results of the analysis showed the absence of an unambiguous statistically significant strong correlation. For the SBAS-InSAR monitoring data on the ascending orbit, the Spearman coefficient (RSpearman) reached the maximum negative value of a moderate relationship of −0.36. For the descending orbit, this value was −0.17. Consequently, the established functional relationship between the earthquakes in the study area and the observed dam displacements is more complex, nonlinear, and at this stage cannot be unambiguously confirmed by direct numerical methods.

The cumulative effect of previous strong earthquakes (M = 7.0, 22.01.2024, 320 km; M = 5.0, 04.03.2024, 57 km) could have significantly aggravated the existing deformations and contributed to subsequent failures (30.03.2024). However, it is important to note that the peak ground acceleration (PGA) from these events did not exceed 0.083 g. This is significantly lower than the design critical limits for the dam structure (0.22 g), indicating that these earthquakes were probably not the direct cause of the failure, given its initial integrity.

Displacement velocity gradients. Decomposition of LOS displacements of the dam surface into horizontal and vertical components allowed us to construct maps of normalized gradients of displacement rate changes in plan. (Figure 21).

Anomalous values of displacements and changes in their gradients were revealed in the central part of the dam compared to the flanks. This area is under the maximum hydrostatic pressure of water from the reservoir, which makes it most susceptible to internal erosion processes (suffusion, cavitation, undermining).

The key parameter of soil shear strength is the angle of internal friction. According to laboratory analysis data for borehole #1, for the dam body it is 26° at natural humidity and 17° in a water-saturated state. For the dam foundation, these values are 30° and 27°, respectively. Thus, with water saturation, there is a significant decrease in the effective friction resistance of the dam soils. This is due to the destruction of structural bonds and an increase in pore pressure for cohesive soils (loams), as well as the elimination of apparent adhesion and the influence of pore pressure for non-cohesive soils (sands). We assume that a combination of abnormal displacements, excessive waterlogging, and moderate correlation with the micro seismicity of the area could have caused the dam breakthrough in this central part.

The study of the dynamics of displacements at other dams made it possible to establish characteristic, repeating deformation patterns, which, in turn, made it possible to identify specific features that preceded the breakthrough at the Voroshilov Reservoir. In our opinion, the pronounced wave-like nature of the dynamics of displacements in combination with a sharp increase in the amplitude of displacements for earth dams of this type can be a convincing indicator of a critical increase in moisture saturation and a potential harbinger of an impending breakthrough or destruction of the structure. In addition, the unstable response of the graphs of the dynamics of deformations to seismic events in the region is a critically important feature that requires special attention when monitoring dams in seismically hazardous areas. The proposed method for assessing the state of the hydraulic structures based on a long-term analysis of the dynamics of displacements, although it does not replace traditional methods of ground monitoring, can serve as an effective tool for ranking objects by risk and determining the priority of detailed surveys.

Comparison with cases of large dam failures emphasizes that the mechanism of destruction of the Voroshilov reservoir contains features typical of embankment structures. These include a high degree of water saturation of the dam body and a decrease in the strength characteristics of the foundation due to filtration processes (like the Sardoba (Uzbekistan, 2020) (Xiao et al., 2022) and Cadia tailings dam (Australia, 2018) (Minhui et al., 2019) accidents). Moreover, a study of the Oroville dam failure (USA, 2017) demonstrates that even structures with concrete elements can fail in the presence of hydrodynamic loads and erosion processes in the foundation (Koskinas et al., 2019; Zhang et al., 2024).

All the listed accidents are characterized by a combination of geotechnical defects, degradation of the physical and mechanical properties of soils, and insufficient engineering monitoring. The scale of the consequences depends on the volume of the reservoir and the terrain features, but the risk structure remains comparable. The mechanism of destruction of the Voroshilov reservoir also shows: a high degree of saturation of the dam body, weakening of the

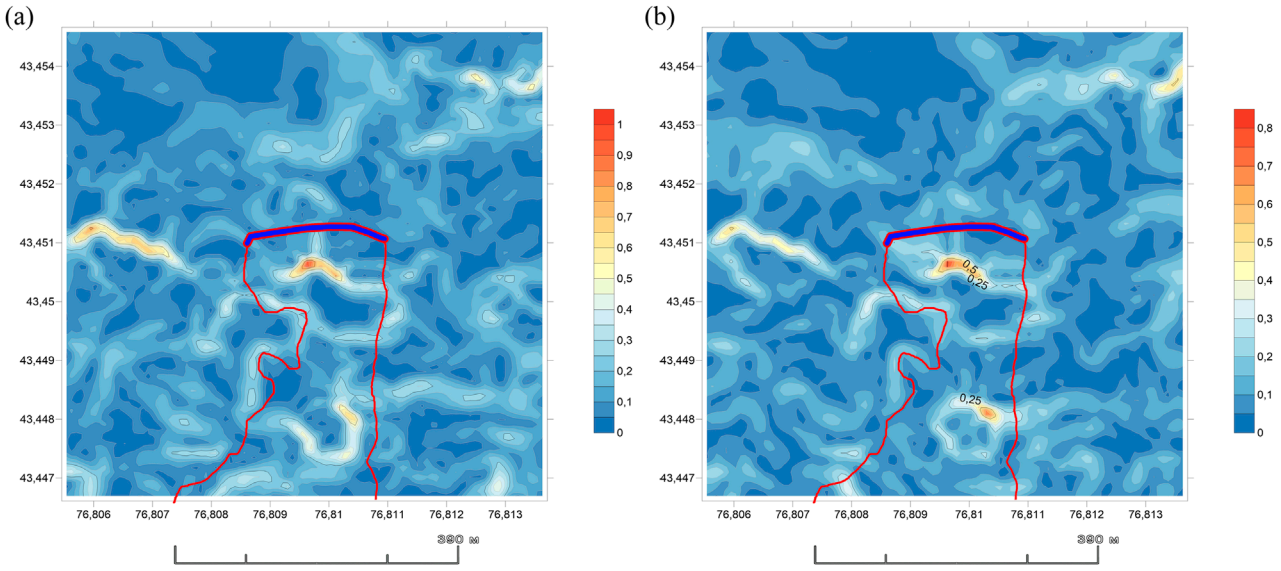

FIGURE 21
Schematic maps of normalized gradients of displacement rate of the Voroshilov Dam in plan: **(a)** gradient of vertical displacements, **(b)** gradient of horizontal displacements. The red line is the reservoir contour; the red and blue line is the dam.

foundation, development of filtration processes, which corresponds to typical scenarios of degradation of earth structures.

Thus, the identified patterns of destruction coincide with international scenarios, confirming the relevance of introducing combined monitoring to identify precursors of accidents for such hydraulic structures.

5 Conclusion

The conducted comprehensive InSAR and GPR study revealed the key factors of the Voroshilov Reservoir dam break: critically high moisture saturation of the dam body (even after drainage), which provoked intense filtration, soil erosion and progressive internal erosion, leading to destruction. The critical increase in moisture saturation also contributed to the growth of pore pressure, reducing the effective stress in the soil. This led to a decrease in the stability of the dam material and created the prerequisites for sudden deformations or even liquefaction of the soil. These findings are convincingly confirmed by the results of InSAR monitoring of the deformation behavior of the dam. The graphs of deformation processes reflect the increasing instability of the technical condition. Since the spring of 2022, abnormal positive displacements with an amplitude of up to 30 mm have been recorded, which is probably due to progressive moisture saturation and swelling of the soil. The influence of microseismic activity in the region should not be underestimated. A clear trend of increasing deformations of the dam body after each seismic event is observed. The culmination was two powerful seismic shocks in January and March 2024, which, with a high degree of probability, served as a direct trigger for the final failure of the dam.

Although the dam failure is a multifactorial event, the totality of the data obtained allows us to assume with a high degree of confidence that the key role was played by massive water filtration through the dam body, potential soil sliding and a significant period of operation of the facility, which caused the accumulation of defects. The results of this study convincingly demonstrate the critical importance of regular and comprehensive assessment of the technical condition of the hydraulic structures, including the use of ground and remote sensing methods. Timely preventive repair work based on the results of such monitoring can significantly reduce the potential damage from the harmful effects of water and prevent catastrophic accidents. Considering the results of the comprehensive monitoring and the identified factors that led to the destruction of the Voroshilov Reservoir dam, it is advisable to recommend:

- Continue developing integrated methods for monitoring hydraulic structures that combine remote sensing (InSAR, aerolidar) with ground-based geophysical surveys (GPR, geodesy, filtration control).
- Strengthen research to increase the spatial resolution of satellite monitoring of small and medium dams, including the use of high-resolution radar data (e.g., TerraSAR-X, COSMO-SkyMed) and the integration of data from several satellites to increase the density of measurements.
- Expand the comparative analysis of the dynamics of displacements in similar dams in the region to identify typical deformation patterns preceding accidents to create an early warning system.
- Conduct research on modeling seismic impact on the deformation behavior of dams in seismically hazardous areas, including numerical modeling of the reaction of soils and the dam body.
- Recommend the introduction of regular remote monitoring of the state of dams in Kazakhstan, considering the climatic,

geotechnical and seismic features of the territories, to minimize the risk of destruction and increase the reliability of hydraulic structures.

Data availability statement

The original contributions presented in the study are included in the article/supplementary material, further inquiries can be directed to the corresponding author.

Author contributions

DT: Writing – review and editing, Methodology, Validation, Writing – original draft, Visualization, Conceptualization. AV: Writing – review and editing, Methodology, Conceptualization, Validation. TD: Writing – original draft, Visualization. OK: Formal Analysis, Writing – original draft, Visualization. GJ: Supervision, Writing – original draft, Funding acquisition.

Funding

The author(s) declare that financial support was received for the research and/or publication of this article. This research has is funded by the Science Committee of the Ministry of Science and Higher Education of the Republic of Kazakhstan (Grant No. AP19680060) "Development of a method for assessing the technical condition of water facilities based on ground-space data and geospatial modeling".

Acknowledgments

The authors express their gratitude to the head of the production site "Ile" of the State Communal Enterprise on the Right of Economic Management "Almatyoblvodkhoz" of the state institution "Department of Water Resources and Irrigation of the Almaty Region" Beisembaev Zhenisbek Zhumabekovich for the provided materials.

Conflict of interest

The authors declare that the research was conducted in the absence of any commercial or financial relationships that could be construed as a potential conflict of interest.

Generative AI statement

The author(s) declare that no Generative AI was used in the creation of this manuscript.

Publisher's note

References

Abdikan, S., Arıkan, M., Sanli, F. B., and Cakir, Z. (2014). Monitoring of coal mining subsidence in peri-urban area of Zonguldak city (NW Turkey) with persistent scatterer interferometry using ALOS-PALSAR. *Environ. Earth Sci.* 71 (9), 4081–4089. doi:10.1007/s12665-013-2793-1

Acosta, L. E., de Lacy, M. C., Ramos, M. I., Cano, J. P., Herrera, A. M., Avilés, M., et al. (2018). Displacements study of an Earth fill dam based on high precision geodetic monitoring and numerical modeling. *Sensors Switz.* 18 (5), 1369. doi:10.3390/s18051369

Aditiya, A., and Ito, T. (2023). Present-day land subsidence over semarang revealed by time series InSAR new small baseline subset technique. *Int. J. Appl. Earth Observation Geoinformation* 125, 103579. doi:10.1016/j.jag.2023.103579

Allias Omar, S. M., Wan Ariffin, W. N. H., Mohd Sidek, L., Basri, H., Moh Khambali, M. H., and Ahmed, A. N. (2022). Hydrological analysis of batu dam, Malaysia in the urban area: flood and failure analysis preparing for climate change. *Int. J. Environ. Res. Public Health* 19 (24), 16530. doi:10.3390/ijerph192416530

Antoine, R., Fauchard, C., Fargier, Y., and Durand, E. (2015). Detection of leakage areas in an Earth embankment from GPR measurements and permeability logging. *Int. J. Geophys.* 2015, 1–9. doi:10.1155/2015/610172

Aureli, F., Maranzoni, A., and Petaccia, G. (2021). Review of historical dam-break events and laboratory tests on real topography for the validation of numerical models. *WaterSwitzerl.* 13 (Issue 14), 1968. doi:10.3390/w13141968

Bayaraa, M., Sheil, B., and Rossi, C. (2022). InSAR and numerical modelling for tailings dam monitoring – the cadia failure case study. *Geotechnique* 74 (10), 985–1003. doi:10.1680/jgeot.21.00399

Bayramov, E., Sydyk, N., Nurakynov, S., Yelisseyeva, A., Neafie, J., and Aliyeva, S. (2024). Quantitative assessment of urban surface deformation risks from tectonic and seismic activities using multitemporal microwave satellite remote sensing: a case study of Almaty city and its surroundings in Kazakhstan. *Front. Built Environ.* 10. doi:10.3389/fbuil.2024.1502403

Betti, A., Crisostomi, E., Paolinelli, G., Piazzi, A., Ruffini, F., and Tucci, M. (2021). Condition monitoring and predictive maintenance methodologies for hydropower plants equipment. *Renew. Energy* 171, 246–253. doi:10.1016/j.renene.2021.02.102

Crosetto, M., Monserrat, O., Cuevas-González, M., Devanthéry, N., and Crippa, B. (2016). Persistent scatterer interferometry: a review. *ISPRS J. Photogrammetry Remote Sens.* 115, 78–89. doi:10.1016/j.isprsjprs.2015.10.011

Davis, J. L., and Annan, A. P. (1986). High-resolution sounding using ground-probing radar. *Geosci. Can.* 13 (3). Available online at: https://journals.lib.unb.ca/index.php/GC/article/view/3467/3981.

Dwitya, R., Hendrianto Pratomo, A., Agung Cahyadi, T., Rianto Budi Nugroho, A., Prio Utomo, D., and Sulo, C. (2024). Slope stability monitoring of hydroelectric dam and upstream watershed areas utilizing satellite interferometric synthetic aperture radar (InSAR). *IOP Conf. Ser. Earth Environ. Sci.* 1339 (1), 012037. doi:10.1088/1755-1315/1339/1/012037

Dyakov, A. Y. (2022). Georadar research of an enclosing dam at a mining waste alluvial storage facility. *Labor Prot. industrial Saf. Saf. Emerg. situations (subsoil use)* 11 (125). doi:10.23670/IRJ.2022.125.56

Fan, Q., Zhang, S., Niu, Y., Zeng, X., Si, J., Li, X., et al. (2024). A non-contact quantitative risk assessment framework for translational highway landslides: Integration of InSAR, geophysical inversion, and numerical simulation. *Eng. Geol.* 343, 107818. doi:10.1016/J.ENGGEO.2024.107818

Gikas, V., and Sakellariou, M. (2008). Settlement analysis of the mornos Earth dam (greece): evidence from numerical modeling and geodetic monitoring. *Eng. Struct.* 30 (11), 3074–3081. doi:10.1016/j.engstruct.2008.03.019

Guzman-Acevedo, G. M., Vazquez-Becerra, G. E., Quintana-Rodriguez, J. A., Gaxiola-Camacho, J. R., Anaya-Diaz, M., Mediano-Martinez, J. C., et al. (2024). Structural health monitoring and risk assessment of bridges integrating InSAR and a calibrated FE model. *Structures* 63, 106353. doi:10.1016/J.ISTRUC.2024.106353

Hanssen, R. F. (2001). *Radar interferometry: data interpretation and error analysis (remote sensing and digital image processing)*. Springer.

Hrysiewicz, A., Holohan, E. P., Donohue, S., and Cushnan, H. (2023). SAR and InSAR data linked to soil moisture changes on a temperate raised peatland subjected to a wildfire. *Remote Sens. Environ.* 291, 113516. doi:10.1016/j.rse.2023.113516

Hu, J., Li, Z. W., Ding, X. L., Zhu, J. J., Zhang, L., and Sun, Q. (2014). Resolving three-dimensional surface displacements from InSAR measurements: a review. *Earth-Science Rev.* 133, 1–17. doi:10.1016/j.earscirev.2014.02.005

Huang, W. K., Li, S. P., Tan, C., and Lu, P. Y. (2024). Application of ground penetrating radar in potential hazards detection of levee. *J. Phys. Conf. Ser.* 2887 (1), 012062. doi:10.1088/1742-6596/2887/1/012062

International Commission on Large Dams (2020). ICOLD. Dam legislation: final report.

Jänichen, J., Ziemer, J., Wolsza, M., Klöpper, D., Weltmann, S., Wicker, C., et al. (2025). Towards operational dam monitoring with PS-InSAR and electronic corner reflectors. *Remote Sens.* 17 (7), 1318. doi:10.3390/rs17071318

Jo, M. J., Jung, H. S., and Won, J. S. (2015). Detecting the source location of recent summit inflation via three-dimensional InSAR observation of Kīlauea volcano. *Remote Sens.* 7 (11), 14386–14402. doi:10.3390/rs71114386

Kalkan, Y. (2014). Geodetic deformation monitoring of ataturk dam in Turkey. *Arabian J. Geosciences* 7 (1), 397–405. doi:10.1007/s12517-012-0765-5

Koohmishi, M., Kaewunruen, S., Chang, L., and Guo, Y. (2024). Advancing railway track health monitoring: integrating GPR, InSAR and machine learning for enhanced asset management. *Automation Constr.* 162, 105378. doi:10.1016/j.autcon.2024.105378

Koskinas, A., Tegos, A., Tsira, P., Dimitriadis, P., Iliopoulou, T., Papanicolaou, P., et al. (2019). Insights into the oroville dam 2017 spillway incident. *Geosci. Switz.* 9 (1), 37. doi:10.3390/geosciences9010037

Leigh, C., Alsibai, O., Hyndman, R. J., Kandanaarachchi, S., King, O. C., McGree, J. M., et al. (2019). A framework for automated anomaly detection in high frequency water-quality data from *in situ* sensors. *Sci. Total Environ.* 664, 885–898. doi:10.1016/j.scitotenv.2019.02.085

Li, C., Ding, L., Guo, Z., Wang, Z., Wei, L., Zheng, Y., et al. (2025). Spatiotemporal evolution of surface deformation based on MT-InSAR and mechanism analysis along zhengzhou metro, China. *Tunn. Undergr. Space Technol.* 156, 106182. doi:10.1016/J.TUST.2024.106182

Liu, Y., Cao, W., Shi, Z., Yue, Q., Chen, T., Tian, L., et al. (2023). Evaluation of post-tunneling aging buildings using the InSAR nonuniform settlement index. *Remote Sens.* 15 (14), 3467. doi:10.3390/rs15143467

Loperte, A., Bavusi, M., Cerverizzo, G., Lapenna, V., and Soldovieri, F. (2011). Ground penetrating radar in dam monitoring: the test case of acerenza (southern Italy). *Int. J. Geophys.* 2011, 1–9. doi:10.1155/2011/654194

Ma, P., Zheng, Y., Zhang, Z., Wu, Z., and Yu, C. (2022). Building risk monitoring and prediction using integrated multi-temporal InSAR and numerical modeling techniques. *Int. J. Appl. Earth Observation Geoinformation* 114, 103076. doi:10.1016/j.jag.2022.103076

MacChiarulo, V., Milillo, P., Blenkinsopp, C., Reale, C., and Giardina, G. (2021). Multi-temporal InSAR for transport infrastructure monitoring: recent trends and challenges. *Proc. Institution Civ. Eng. Bridge Eng.* 176 (2), 92–117. doi:10.1680/jbren.21.00039

Marchamalo-Sacristán, M., Ruiz-Armenteros, A. M., Lamas-Fernández, F., González-Rodrigo, B., Martínez-Marín, R., Delgado-Blasco, J. M., et al. (2023). MT-InSAR and dam modeling for the comprehensive monitoring of an earth-fill dam: the case of the benínar dam (almería, Spain). *Remote Sens.* 15 (11). doi:10.3390/rs15112802

Minhui, S., Chua, T., and Garthwaite, M. (2019). Leveraging open-access remote sensing imagery to monitor dam infrastructure: case study of the cadia tailings dam collapse, Australia. Available online at: https://github.com/dbekaert/StaMPS/.

Nasika, C., Díez, P., Gerard, P., Massart, T. J., and Zlotnik, S. (2022). Towards real time assessment of earthfill dams *via* model order reduction. *Finite Elem. Analysis Des.* 199, 103666. doi:10.1016/j.finel.2021.103666

Nestorović, Ž., Trifković, M., and Kuburić, M. (2024). Geodetic monitoring of large dams – characteristics and significance. *Zb. Rad. Trinaestog Međunar. Naučno-Stručnog Savetovanja Ocena Stanja, Održavanje i Sanacija Građev. Objekata*, 326–330. doi:10.46793/SGISXIII.32ZN

Ng, A. H. M., Wen, B., Ma, Y., Guo, L., Dai, Y., Wang, H., et al. (2024). Integrating spatial modeling-assisted InSAR phase unwrapping with temporal analysis for advanced mine subsidence time series mapping. *Int. J. Appl. Earth Observation Geoinformation* 133, 104143. doi:10.1016/J.JAG.2024.104143

Pang, Z., Jin, Q., Fan, P., Jiang, W., Lv, J., Zhang, P., et al. (2023). Deformation monitoring and analysis of reservoir dams based on SBAS-InSAR technology—banqiao reservoir. *Remote Sens.* 15 (12), 3062. doi:10.3390/rs15123062

Pengchao, C. (2025). Advancements and future outlook of safety monitoring, inspection and assessment technologies for oil and gas pipeline networks. *J. Pipeline Sci. Eng.*, 100267. doi:10.1016/J.JPSE.2025.100267

Piter, A., Haghshenas Haghighi, M., and Motagh, M. (2024). Challenges and opportunities of Sentinel-1 InSAR for transport infrastructure monitoring. *PFG – J. Photogrammetry, Remote Sens. Geoinformation Sci.* 92 (5), 609–627. doi:10.1007/s41064-024-00314-x

Ruiz, J. J., Lemmetyinen, J., Kontu, A., Tarvainen, R., Vehmas, R., Pulliainen, J., et al. (2022). Investigation of environmental effects on coherence loss in SAR interferometry for snow water equivalent retrieval. *IEEE Trans. Geoscience Remote Sens.* 60, 1–15. doi:10.1109/TGRS.2022.3223760

Ruiz-Armenteros, A. M., Marchamalo-Sacrsitán, M., Bakoň, M., Lamas-Fernández, F., Delgado, J. M., Sánchez-Ballesteros, V., et al. (2021). Monitoring of an embankment dam in southern Spain based on Sentinel-1 time-series InSAR. *Procedia Comput. Sci.* 181, 353–359. doi:10.1016/j.procs.2021.01.178

Silacheva, N. V., Kulbayeva, U. K., and Kravchenko, N. A. (2018). Probabilistic seismic hazard assessment of Kazakhstan and Almaty city in peak ground accelerations. *Geodesy Geodyn.* 9 (2), 131–141. doi:10.1016/j.geog.2017.11.002

Tanajewski, D., and Bakuła, M. (2016). Application of ground penetrating radar surveys and GPS surveys for monitoring the condition of levees and dykes. *Acta Geophys.* 64 (Issue 4), 1093–1111. doi:10.1515/acgeo-2016-0006

Tang, Z., Chen, Z., Bao, Y., and Li, H. (2019). Convolutional neural network-based data anomaly detection method using multiple information for structural health monitoring. *Struct. Control Health Monit.* 26 (1), e2296. doi:10.1002/stc.2296

Teixeira, A. C., Bakon, M., Perissin, D., and Sousa, J. J. (2024). InSAR analysis of partially coherent targets in a subsidence deformation: a case study of maceió. *Remote Sens.* 16 (20), 3806. doi:10.3390/rs16203806

Tian, F., Zhang, W., Zhu, H.-H., Wang, C., Chang, F.-N., Li, H.-Z., et al. (2025). Multi-temporal InSAR-based landslide dynamic susceptibility mapping of fengjie county, three gorges reservoir area, China. *J. Rock Mech. Geotechnical Eng.* doi:10.1016/J.JRMGE.2025.01.012

Tzouvaras, M., Danezis, C., and Hadjimitsis, D. G. (2020). Differential SAR interferometry using sentinel-1 imagery-limitations in monitoring fast moving landslides: the case study of Cyprus. *Geosci. Switz.* 10 (6), 236. doi:10.3390/geosciences10060236

Wang, P., Xing, C., and Pan, X. (2020a). Reservoir dam surface deformation monitoring by differential GB-inSAR based on image subsets. *Sensors Switz.* 20 (2), 396. doi:10.3390/s20020396

Wang, Y., Bai, Z., Lin, Y., Li, Y., and Shen, W. (2020b). Sentinel-1 Quasi-PS InSAR for identification and monitoring of landslide deformation. *IET Conf. Proc.* 2020 (9), 946–949. doi:10.1049/icp.2021.0776

Wang, Y., Shen, D., Chen, J., Pei, L., Li, Y., Lu, X., et al. (2020c). Research and application of a smart monitoring system to monitor the deformation of a dam and a slope. *Adv. Civ. Eng.* 2020. doi:10.1155/2020/9709417

Wang, L., Xie, L., and Xi, C. (2024). Improved artificial bee colony algorithm for pressure source parameter inversion of sakurajima volcano from InSAR data. *Geodesy Geodyn.* 15, 635–641. doi:10.1016/j.geog.2024.05.004

Xiao, R., Jiang, M., Li, Z., and He, X. (2022). New insights into the 2020 sardoba dam failure in Uzbekistan from Earth observation. *Int. J. Appl. Earth Observation Geoinformation* 107, 102705. doi:10.1016/j.jag.2022.102705

Xiong, S. H., Wang, Z. P., Li, G., Skibniewski, M. J., and Chen, Z. S. (2024). Prediction of airport runway settlement using an integrated SBAS-InSAR and BP-EnKF approach. *Inf. Sci.* 665, 120376. doi:10.1016/j.ins.2024.120376

Xue, B., Gao, J., Hu, S., Li, Y., Chen, J., and Pang, R. (2023). Ground penetrating radar image recognition for Earth dam disease based on you only look once v5s algorithm. *WaterSwitzerl.* 15 (19), 3506. doi:10.3390/w15193506

Yang, K., Yan, L., Huang, G., Chen, C., and Wu, Z. (2016). Monitoring building deformation with InSAR: experiments and validation. *Sensors Switz.* 16 (12), 2182. doi:10.3390/s16122182

Zakharov, A., and Zakharova, L. (2023). An influence of snow covers on the radar interferometry observations of industrial infrastructure: norilsk thermal power plant case. *Remote Sens.* 15 (3), 654. doi:10.3390/rs15030654

Zhang, X., Wang, C., Chen, X., Dong, J., Hu, M., and Liu, S. (2024). Insights into the cause of the oroville dam spillway failure, 2017, California. *Environ. Sci. Pollut. Res.* 31 (14), 21356–21369. doi:10.1007/s11356-024-32462-3

Zhantayev, Z., Kurmanov, B., Breusov, N., Dauren, S., and Alexandr, K. (2013). Ground penetrating radar survey of dam structures of Kazakhstan on example of Aktobe and karatomar water storage basins. *Open J. Geol.* 03 (02), 25–27. doi:10.4236/ojg.2013.32b006

Zheng, Y., Zhao, Z., Zeng, M., Zhou, D., Su, X., and Liu, D. (2024). Monitoring and analysis of surface deformation in the buzhaoba open-pit mine based on SBAS-InSAR technology. *Remote Sens.* 16 (22), 4177. doi:10.3390/rs16224177